Neurotoxicity Research, 2007, VOL. 11(2). pp. 107-130

F.P. Graham Publishing Co.

Neonatal Dopamine Depletion Induces Changes in Morphogenesis and Gene Expression in the Developing Cortex

IRINA N. KRASNOVA[a], ELIZABETH S. BETTS[a,b], ABIOLA DADA[b] AKILAH JEFFERSON[b], BRUCE LADENHEIM[a], KEVIN G. BECKER[c], JEAN LUD CADET[a] AND CHRISTINE F. HOHMANN[b,*]

[a]Molecular Neuropsychiatry Branch, National Institute on Drug Abuse, NIH/DHHS; [b]Department of Biology, Morgan State University; [c]Gene Expression and Genomics Unit, National Institute on Aging, NIH/DHHS, Baltimore, MD 21251 USA. chohmann@jewel.morgan.edu

(Submitted 5 May 2006; Revised 18 August 2006; In final form 12 September 2006)

The mesocorticolimbic dopamine (DA) system is implicated in mental health disorders affecting attention, impulse inhibition and other cognitive functions. It has also been involved in the regulation of cortical morphogenesis. The present study uses focal injections of 6-hydroxydopamine (6-OHDA) into the medial forebrain bundle of BALB/c mice to examine morphological, behavioral and transcriptional responses to selective DA deficit in the fronto-parietal cortex. Mice that received injections of 6-OHDA on postnatal day 1 (PND1) showed reduction in DA levels in their cortices at PND7. Histological analysis at PND120 revealed increased fronto-cortical width, but decreased width of somatosensory parietal cortex. Open field object recognition suggested impaired response inhibition in adult mice after 6-OHDA treatment. Transcriptional analyses using 17K mouse microarrays showed that such lesions caused up-regulation of 100 genes in the cortex at PND7. Notably, among these genes are Sema3A which plays a repulsive role in axonal guidance, RhoD which inhibits dendritic growth and tubulin β5 microtubule subunit. In contrast, 127 genes were down-regulated, including CCTε and CCTζ that play roles in actin and tubulin folding. Thus, neonatal DA depletion affects transcripts involved in control of cytoskeletal formation and pathway finding, instrumental for normal differentiation and synaptogenesis. The observed gene expression changes are consistent with histological cortical and behavioral impairments in the adult mice treated with 6-OHDA on PND1. Our results point towards specific molecular targets that might be involved in disease process mediated by altered developmental DA regulation.

Keywords: Cerebral cortex; Dopamine; Gene expression; 6-Hydroxydopamine; Microarray; Morphology

INTRODUCTION

Building a normal cerebral cortex requires coordinated generation, migration, and differentiation of neurons and glia along with the programmed cell death and formation of appropriate synaptic connections between neurons (Cohen-Cory, 2002; Guillemot *et al.*, 2006; Price *et al.*, 2006). Well synchronized molecular mechanisms and timely expression of specific genes are essential to the formation of cortical layers and the establishment of functional synapses that are critical for normal cortical development (Ziv and Garner, 2004; Guillemot

*Corresponding author: Tel.: 1 (443) 885-4002; FAX: 1 (443) 885-8285; E-mail: chohmann@jewel.morgan.edu
ISSN 1029 8428 print/ ISSN 1476-3524 online.

et al., 2006). The precision required of these events renders the developing cortex extremely sensitive to disruptions by environmental influences as well as genetic predispositions implicated in a number of mental health disorders (Raedler *et al.*, 1998; Rice and Barone, 2000; Johnston *et al.*, 2001; Mick *et al.*, 2002; Durston, 2003). These insults might, in turn, cause persistent problems in cortical ontogeny that later result in impaired cognition, memory and decision making as well as in altered social behaviors in the exposed offspring (Rice and Barone, 2000; Mick *et al.*, 2002).

Dopaminergic afferent projections from the ventral tegmental area (VTA) to the cortex are the most frequently implicated pathways in neurodevelopmental disorders (Johnston *et al.*, 1995; Berger-Sweeney and Hohmann, 1997; Benes *et al.*, 2000). Experimental neonatal depletion of dopamine (DA) is known to result in behavioral deficits which include changes in locomotor activity (Miller *et al.*, 1981; Kalsbeek *et al.*, 1989a) and cognitive functions (Raskin *et al.*, 1983; Archer *et al.*, 1988; Pappas *et al.*, 1992; Luthman *et al.*, 1997). Notably, developmental DA deficits are associated with decreased cortical size and curtailed dendritic growth (Kalsbeek *et al.*, 1987; 1989b; Sherren and Pappas, 2005), in a fashion similar to the neuropathologic abnormalities reported in disorders thought to be secondary to altered DA homeostasis (Johnston *et al.*, 1995; Shenton *et al.*, 2001; Roth and Saykin, 2004). Thus, investigation of the molecular and cellular bases for DA depletion-induced impaired cortical morphogenesis is of paramount importance because it might help to clarify the mechanisms underlying some human neurodevelopmental disorders.

The use of 6-hydroxydopamine (6-OHDA)-induced lesions has been the most popular model for experimental DA depletion in the forebrain. However, some of the lesion studies published to date have several confounds. For example, intracerebroventricular (i.c.v.) injections of 6-OHDA, even if selective for DA, destroy projections not only to the cortex but also to the limbic system (Archer *et al.*, 1988; Luthman *et al.*, 1990). In addition, reactive serotoninergic hypertrophy into DA-denervated cortex has also been shown after i.c.v. applications of the toxin at birth (Blue and Molliver, 1987; Molina-Holgado *et al.*, 1993; Breese *et al.*, 2005). Similarly, thermal lesions to the VTA are also nonselective, inducing reductions in cortical serotonin (5-HT) concentrations (Kalsbeek *et al.*, 1987; 1989a). Altered 5-HT levels in the developing cortex also are known to affect morphogenesis and behavior (Blue *et al.*, 1991; Berger-Sweeney *et al.*, 1998; Boylan *et al.*, 2000; Hohmann *et al.*, 2000). In addition, similarly treated rodents often have reduced brain and body weight (Berger-Sweeney and Hohmann, 1997; Bruno *et al.*, 1998; Breese *et al.*, 2005). Therefore, to isolate potentially deleterious influences of DA depletion on cortical development, we performed the present study using focal injections of 6-OHDA into the medial forebrain bundle (MFB) because it is a more selective animal model of deficient cortical DA. We performed histological analysis in combination with large-scale microarray and RT-PCR approaches in order to determine morphological and transcriptional responses specific to neonatal cortical DA deafferentation. Behavioral tests were conducted to assess the possible cognitive consequences. We show perturbations in the transcriptional developmental programs in the mouse cortex that are consistent with the morphological changes. Our study identifies specific cellular and molecular targets to further investigate dopaminergic morphogenetic influences in cortical development.

MATERIALS AND METHODS

Animals and 6-OHDA Treatment

Male and female BALB/cByJ breeding stock was obtained from Jackson Laboratory (Bar Harbor, ME). All animal procedures were conducted according to the NIH Guide for the Care and Use of Laboratory Animals and were approved by the local Animal Care Committee. BALB/cByJ mice, generated in our breeding colony at Morgan State University, were removed from their mothers within the first 12-20 hours after birth, anesthetized on ice, placed into a specially designed mouse pup holder, and positioned in a stereotaxic apparatus (Kopf, Tujunga, CA). We applied an injection protocol that we empirically developed to perform maximal DA depletion in the cortex without major alterations in other afferent monoamine levels. 6-OHDA hydrobromide (Sigma, St.Louis, MO) was dissolved in 0.9% sterile saline containing 0.2% ascorbic acid to a concentration 10 µg/µl. The solution was prepared fresh prior to injection and kept on ice in order to minimize oxidation.

Injections were made into the MFB near the diagonal band of Broca, horizontal limb, similar to previously described (Hohmann *et al.*, 1988; Hohmann and Berger-Sweeney, 1998). Coordinates for the injections were measured using the sinuses underlying the midline and frontonasal skull suture, and 0.6 microliters (= 6 µg) of 6-OHDA solution was injected into each hemisphere. On each side, a 27 gauge needle was lowered into the brain through skin and skull 2 mm anterior to the frontonasal suture and 1.5 mm lateral to midline, at an angle of 15° horizontally and 58° vertically. 6-OHDA was slowly administered in three injections (0.2 µl each) at a depth of 4.0 mm (1st injection), 3.5 mm (2nd injection), or 3 mm (3d injection) along the posterior to anterior trajectory of the needle tract in the forebrain. Litter mates, injected with vehicle, served as controls for all experiments. Each group contained mice from at least three different litters. After the injections, pups were re-warmed to normal body temperature on a heating pad and returned to their mothers. For HPLC and microarray analysis, male mice were sacrificed by cervical dislocation on PND7, their brains were rapidly removed from the skulls and dissected on an ice-cooled plate. The samples were taken from dorsal fronto-parietal cortex to closely resemble the cortical areas examined histologically. In addition, striata were dissected out and used for HPLC analysis. Tissue samples were immediately frozen on dry ice, weighed, and processed for HPLC or RNA isolation as described below. For behavioral and histology experiments, male mice were weaned on PND30 and group housed with littermates until the start of behavioral testing.

HPLC Analysis

Cortical samples (N=8 per group) were ultrasonicated in 0.1 M perchloric acid containing 10 ng/mg of internal standard dihydroxybenzilamine, then centrifuged at 20,000g for 10 min. Concentrations of norepinephrine (NE), DA, 3,4-dihydroxyphenylacetic acid (DOPAC), homovanillic acid (HVA), 5-HT, and 5-hydroxyindoleacetic acid (5-HIAA) in cortical and striatal tissue extracts of 6-OHDA and vehicle-treated mice were measured by HPLC with electrochemical detection as described earlier (Krasnova *et al.*, 2001). Concentrations of NE, DA, DOPAC, HVA, 5-HT, and 5-HIAA were calculated and expressed as pg/mg of tissue weight. Statistical analysis was performed using analysis of variance (ANOVA) followed by Fisher's protected least significant difference (PLSD) (StatView 4.02, SAS Institute, Cary, NC). Differences were considered significant at $p < 0.05$.

Histological Analysis

Histological analysis was performed on 6-OHDA and vehicle-injected male mice (N=5) following behavioral testing (see below). At four months of age, mice were anesthetized with chloral hydrate and perfused transcardially with 0.15 M phosphate buffered saline, pH 7.4 (PBS) followed by 4% paraformaldehyde in PBS. After perfusion, the brains were removed, post-fixed in the perfusion solution for 4-8 hours, immersed in 20% sucrose in PBS for cryoprotection overnight, frozen in isopentane and stored at -80°C. Quantitative morphological assessments were performed as described in detail before (Hohmann and Berger-Sweeney, 1998; Hohmann *et al.*, 2000). Briefly, Nissl stained coronal 50 µm-thick sections through comparable levels of frontal cortex [FC] (level of first appearance of the anterior commissure), anterior somatosensory cortex [ASSC] (anterior to fimbria fornix), barrel field cortex [BFC] and somatosensory cortex posterior to the barrel field area [PSSC] were selected. Using the AIS Image system (St. Catherine's, Ontario, Canada) images of the sections were digitized and cortical width was measured, bilaterally, in an approximately 3 mm wide area of neocortex. For each section, cortical and laminar thickness (total cortex, layer VI, V, IV and II/III) measurements were taken at four separate positions in this sample area. For frontal cortex, measurements were taken medially to the rhinal fissure and laterally to the cingulate cortex. In the other areas samples were taken, just lateral to the agranular motor cortex, in the dorsal parietal cortex. Means of these individual measurements for each section were used for statistical analysis by unpaired t-test, comparing 6-OHDA versus vehicle-treated cortices (StatView 4.02). Criteria for significance were set at $p \leq 0.05$.

Behavioral Testing

Beginning at PND 90, 6-OHDA-lesioned, vehicle-injected control and age-matched normal male mice (N=10) were handled for one week before being subjected to the Neurological Test Battery followed by an Open Field Object Recognition Task (OFOR).

A. Neurological Test Battery

The Neurological Test Battery is akin to a clinical neurological examination for mice and assesses basic sensorimotor abilities such as the righting reflex, placing reflex, grip strength and ability to walk across a narrow, round beam. For all assessments, the experimenter was blind to the condition of the mice (6-OHDA-lesioned or vehicle-treated littermates). All tests were performed in triplicate on all mice, prior to the onset of behavioral testing, and the average scores for each animal were used for subsequent analysis.

For the righting reflex, mice were lowered by their tails toward a flat horizontal surface while the experimenter attempted to place the mouse' back onto this surface. The ability of mice to turn around and land on their paws was rated on a scale of 1-4. If a mouse could not be turned on its back, it was given a score of 4, a more sluggish response in righting itself was given a score of 3 and 2, progressively; mice unable to right themselves or those who responded with disorientation after righting themselves would have received a score of 1. Impairments in the righting reflex suggest deficits in proprioception or equilibrium. For the placing reflex, mice were lowered by their tail toward the grid of the cage top; their readiness to stretch out their front paws towards the surface, as they neared it, was rated on a scale from 1-4. A score of 4 was given to a mouse that immediately stretched its paws as it neared the surface; a score of 3 and 2 indicated a progressively delayed response and a score of 1 would have signified that the animal landed head first on the surface. Deficits in the placing reflex suggest sensorimotor rather than visual impairment, as the animal's whiskers touch the surface prior to the body. For grip strength, mice were allowed first to attach to the grid of the cage top, then were pulled away by their tail; the strength of attachment to the cage top was assessed on a scale of 1-4. A strong resistance to being pulled away from the cage top equaled a score of 4, a weakened resistance a score of 3 and 2, progressively, and no resistance a score of 1. Reduced grip strength is an indicator of reduced muscle strength or overall ill health.

For performance of the beam-walking task, the "beam" (a 5 ml pipette) was stretched between the home cage and a support at the opposite end of the beam. A mouse was placed on a platform near the far end of the beam and allowed to move toward the home cage, which is a strong motivator. We measured the amount of time, up to a maximum of 125 seconds, taken by each mouse to cross the beam and enter the home cage. Mice that did not cross the beam to their home cage within 125 seconds were removed from the task and given the maximum score of 4. In addition, we rated the ability of the mouse to cross smoothly without losing grip on a scale from 1-4, with 4 being the worst score. Each time a mouse fell off the beam or just held on to the beam by one or two paws, its score increased by one point up to a maximum of 4. The beam-walking test assesses both motor coordination and anxiety (reluctance to cross the beam).

B. OFOR

This task was adapted from a test developed by Ricceri *et al.* (1999) in accordance with parameters introduced by Poucet (1989). The task is performed in a round enclosure of approximately 90 cm in diameter, surrounded by walls of about 25 cm in height that lean outward at a slight angle of about 15 degrees (commercial plastic baby pool). The entire enclosure is painted black to increase visibility of white mice; quadrants are marked on the floor with white lines. Mice were videotaped during the performance of all aspects of the task and all measurements were conducted on a Dell Pentium computer using Observer Video-Pro (Noldus, Leesburg, VA) software. The objects consisted of Lego constructions of various shapes and colors. The apparatus was wiped with an alcohol/water solution between subjects to reduce odor cues.

In the first session (S1), mice were placed into the enclosure without objects, to assess open field behaviors including locomotor activity and rearing. During sessions 2-4 (S2-S4), 5 objects of different shapes and colors were placed at set locations in the enclosure and the amount of time a mouse explored the objects was scored. Exploration consisted of either "whisking" or sniffing the object, exploration with forepaws or climbing onto the object. In session 5 (S5), objects 1 and 5 (displaced objects (DO)) were moved to a new location; their position was maintained in session 6 (S6). In session 7 (S7), object 3 was replaced with a new object 6 (substituted object (SO)). At each session mice

were placed into the enclosure for 6 minutes with 3-minute intervals between sessions. The experimenter recorded the time spent with each object. In S5-7, control mice are expected to increase exploration, especially of the displaced or new objects, compared to the prior sessions. Thus, time spent with the displaced object (DO) compared to the other objects (non-displaced objects (NDO)) in S5 is used to measure the mouse' spatial recognition and memory. In S7, time spent with the new object (substituted object (SO)) compared to the other objects (non-substituted objects (NSO)) signals the animal's ability to recognize and respond to novelty. DO/NDO and SO/NSO scores were calculated according to a formula devised by Ricceri *et al.* (1999): DO = mean time spent with displaced objects in S5 minus mean time spent with the same objects in S4; NDO = mean time spent with non-displaced objects in S5 minus mean time with the same objects in S4. SO = mean time spent with the substituted object (object 6) in S7 minus mean time spent with the object previously in this position (object 3) in S6. NSO = mean time spent with non-substituted objects in S7 minus mean time with the same objects in S6. Group values were compared statistically by factorial ANOVA with Fisher's *post-hoc* test and also by repeated measures ANOVA and unpaired *t*-test for DO versus NDO exploration in sessions 5 through 7. All behavioral statistical analyses were performed using StatView 4.02. The null hypothesis was rejected at the $p \leq 0.05$ level.

RNA Isolation and Microarray Hybridization

Total RNA was isolated from individual samples of cerebral cortices of 6-OHDA or vehicle-treated male animals using RNeasy Mini Kit (QIAGEN, Valencia, CA) in accordance with the manufacturer's protocol. RNA concentrations were determined by UV spectrophotometry and RNA integrity was confirmed using denaturing 1.0% agarose-formaldehyde gel. Samples were stored at -70°C.

Microarray experiments were performed using single channel labeling ^{33}P nylon membrane-based cDNA microarrays containing 16,896 features, which include 12,341 unique mouse genes and expressed sequence tags (ESTs) (Mouse 17K array sets) provided by the Gene Expression and Genomics Unit, National Institute of Aging, NIH (Baltimore, MD). Array hybridization and data analysis were supervised by Gene Expression and Genomics Unit. Protocols on array printing, labeling, and hybridization as well as information on software packages are available at the Gene Expression and Genomics Unit website (www.grc.nia.nih.gov/branches/rrb/dna/dna.htm). Each mouse's cortical RNA was processed and run on a separate microarray membrane. Briefly, for probing of microarray membranes, 10 µg of total RNA isolated from cortices of vehicle- and 6-OHDA-treated mice (N=7 samples per group) were reverse-transcribed using SuperScript II reverse transcriptase (Invitrogen, Carlsbad, CA) and labeled with [α-^{33}P]-dCTP (Amersham, Piscataway, NJ). Microarray membranes were pre-hybridized in 4 ml hybridization buffer containing 3.2 ml of Microhyb (Invitrogen), 0.8 ml of 50% dextran sulfate, 100 µl of 10 mg/ml denatured human C_ot DNA (Invitrogen) and 100 µl of 8 mg/ml denatured poly(dA) (Sigma) for 2 hours at 55°C. Radiolabeled cDNA probes were purified using Mico Bio-Spin P-30 Tris chromatography columns (Bio-Rad, Hercules, CA), heat-denatured and hybridized with microarray membranes using 4 ml of fresh hybridization buffer for 18 hours at 55°C. After three high-stringency washes in 2X SSC and 0.1% SDS for 15 min at 55°C, the membranes were exposed to a phosphor screen for 3 days and images were scanned using a Storm 860 PhosphoImager (Molecular Dynamics, Inc., Sunnyvale, CA) with 50 µm resolution. Hybridization intensities of array spots were quantified using ArrayPro analysis software for Windows NT (Media Cybernetics, CA, USA) and then stored as MS Excel (Microsoft, Redmond, WA) spreadsheets.

Statistical Analysis of Microarray Data

We followed MIAME (Minimum Information About a Microarray Experiment) guidelines for the presentation of our results (Brazma *et al.*, 2001). Study design and data analysis were in cooperation with the Gene Expression and Genomics Unit, NIA, NIH. To minimize bias due to individual genetic background differences, treated animal groups were represented by 7 mice. Nonspecific uniform background across entire arrays due to experimental variation was normalized in MS Excel using global normalization. The data value for each spot on each membrane was divided by the median intensity value of that membrane to obtain

a normalized intensity value. Intensity data for each gene were logarithmically transformed. To eliminate noise from low level expression, we filtered out all genes whose average normalized intensity between treatment and control was less than zero. We applied the criteria that the average normalized intensities of treatment and control is larger than zero:

$$\frac{\log \text{treatment intensity} + \log \text{control intensity}}{2} > 0$$

Thus, spurious ratios from background level intensity genes were eliminated. That was the case for less than 20 genes. For further analysis, the data were imported into GeneSpring (version 5.2, Silcon Genetics, Redwood City, CA) by MS Excel spreadsheet formatted as a tab-delimited text file. Changes in gene expression after 6-OHDA treatment were then calculated by ANOVA statistical analysis using GeneSpring. Criteria for significance were set at $p < 0.05$.

Functional grouping analysis for significantly changed genes was performed using DAVID 2.0 Annotation Tool (http://apps1.niaid.nih.gov/david) (Dennis *et al.*, 2003) and supported through literature searches. DAVID is a structured, hierarchical vocabulary to describe gene functions in areas of biological processes, molecular function, and cellular components. Using the standardized DAVID annotation ensured that all gene products have a consistent description that can be employed when comparing other sources of data with this study. To concentrate on changes that could be interpreted in a context of gene function, we included only genes classified using DAVID 2.0 Annotation Tool in the further analysis. We also strengthened statistical confidence by providing evidence of co-regulation of multiple genes that are related by function or pathway. Here we used a software tool, the Expression Analysis Systematic Explorer (EASE; http://david.niaid.nih.gov/david/ease.htm) (Hosack *et al.*, 2003), to assign identified genes to "GO: Biological Process" categories of the Gene Ontology Consortium (www.geneontology.org) and to test statistically (EASE Score, a modified Fisher's exact test) for significant co-regulation (overrepresentation) of identified genes within each biological process category. A hierarchical cluster analysis of the expression with standard correlation 0.95 and distance 0.1 was generated using GeneSpring software.

Quantitative RT-PCR

Total RNA extracted from cortical samples of vehicle and 6-OHDA-treated animals was used for quantitative RT-PCR to confirm some of the results obtained with microarrays as described earlier (Krasnova *et al.*, 2002; 2005). Unpooled total RNA (1 μg) obtained from 7 mice per group was reverse-transcribed with oligo dT primers using Advantage RT for PCR kit (BD Biosciences Clontech, Palo Alto, CA). PCR experiments were performed using light cycler technology and LightCycler FastStart DNA Master SYBR Green I kit (Roche, Indianapolis, IN) according to manufacturer's protocol. Sequences for gene-specific primers corresponding to PCR targets were obtained using LightCycler Probe Design software (Roche). The RT-PCR primer sequences were: glyceraldehyde-3-phosphate dehydrogenase (GAPDH): GTGTGAACCACGAGAAA (upstream), TGGGGTTAGGAACACG (downstream); tubulin β5: GGACTATGGACTCCGT (upstream), CATTGTAGGGCTCGAC (downstream); Ras homolog D (RhoD): TGCGTAAGGACAAGGT (upstream), AATTCTGAGTAATCCGCC (downstream); chaperonin subunit 5 (CCTε): AGCCGAAATATCCTGC (upstream), AGACTCCTTCACCTGT (downstream); chaperonin subunit 6a (CCTζ): ATCATTCCCAAGGTTCT (upstream), GTTGGTGGCGATCACA (downstream); myocyte enhancer factor 2D (MEF2D): AGGAAAAAGATTCAGATCCA (upstream), CTCGTTGTACTCGGTG (downstream); c-Jun: TTGCCCCAACAGATCC (upstream), GCTGCGTTAGCATGAG (downstream); semaphorin 3A (Sema3A): ATTACCTGTGTCACGC (upstream), CTCAAACTCGTGGGTC (downstream). As internal control, 18S cDNA was co-amplified by using primer sequences: GCGCAAATTACCCACT (upstream), ATCCAACTACGAGCTT (downstream). The primers were synthesized and HPLC-purified at the Synthesis and Sequencing Facility of Johns Hopkins University (Baltimore, MD). Negative controls were run concomitantly to confirm the specificity and to verify that no primer dimerization was gen-

erated. The relative standard curve was established with serial dilution of a cDNA solution of unknown concentration that corresponds to a mix of eight randomly picked samples. To confirm the amplification specificity, the PCR products were subjected to a melting curve analysis. Amplification curves were generated by the LightCycler Instrument Quantification program and displayed the fluorescence values versus cycle number. Template concentrations using the relative standard curve were given arbitrary values. The mean 18S concentration was determined once for each cDNA sample and used to normalize all other genes tested from the same cDNA sample. The relative change in gene expression was calculated as the ratio of normalized data over saline. Statistical analysis was done by ANOVA followed by Fisher's PLSD (StatView 4.02). Differences were considered significant if the probability of error was less than 5%.

RESULTS

6-OHDA Lesions

In order to test a possible role for the mesocorticolimbic DA system in the control of cortical development, we used 6-OHDA injections into the MFB at PND1 as a model of cortical DA deficit. To verify the effects of the 6-OHDA lesions on DA levels, we performed HPLC analysis on cortical samples from mice treated with either the neurotoxin or vehicle. 6-OHDA caused marked reduction in DA levels (-78%) 6 days after treatment (FIG. 1A). In contrast, NE, 5-HT, HVA and 5-HIAA concentrations were not significantly affected (FIG. 1A). Concentration of DOPAC in the cortical samples was below detection limit (<1 pg/mg of tissue). Because nigrostriatal DA terminals also project through MFB, we examined the effects of 6-OHDA lesions in the striatum. The neurotoxin also caused a significant decrease in DA levels in the striatum (-38%) (FIG. 1B), but it was less dramatic than in the cortex (FIG. 1A). Concentrations of NE, DOPAC, HVA, 5-HT and 5-HIAA were not significantly changed (FIG. 1B).

Histological Assessments

Qualitative examination of Nissl stained cortical sections from four-month old mice treated with 6-OHDA or vehicle on PND1 showed well-articulated cortical cytoarchitecture in all cases. Injection sites and needle tracts in the base of the forebrain were no longer visible in these adult mice. However, quantitative morphometric analysis revealed striking alterations in cortical width following 6-OHDA lesions that varied significantly according to cortical areas and layers (Table I). In both frontal [FC] and somatosensory cortex [ASSC, BFC and PSSC], layer V was the least affected whereas layer IV was the most prominently altered. 6-OHDA injections resulted in overall decreases in the width of the

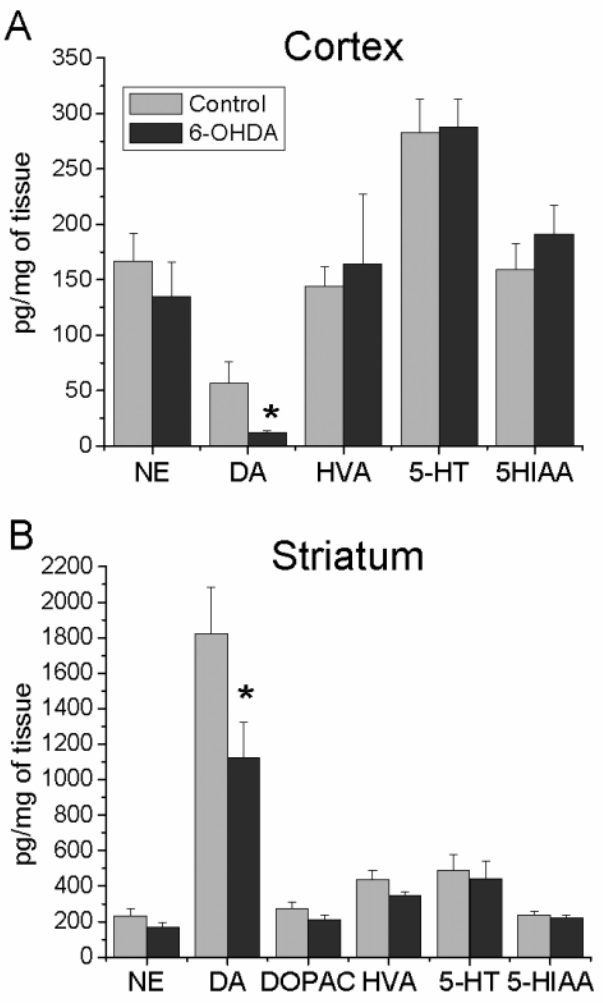

FIGURE 1 Levels of NE, DA, 5-HT and their metabolites in the cerebral cortex (**A**) and striatum (**B**) at PND7 after neonatal 6-OHDA injections into MFB. Neurotoxin induced significant decrease in DA concentrations in both brain regions without affecting NE, 5-HT, DOPAC, HVA and 5-HIAA levels. Values represent means ± SE (pg per mg of tissue) of 7 mice per group. $p < 0.05$ in comparison with vehicle-treated mice.

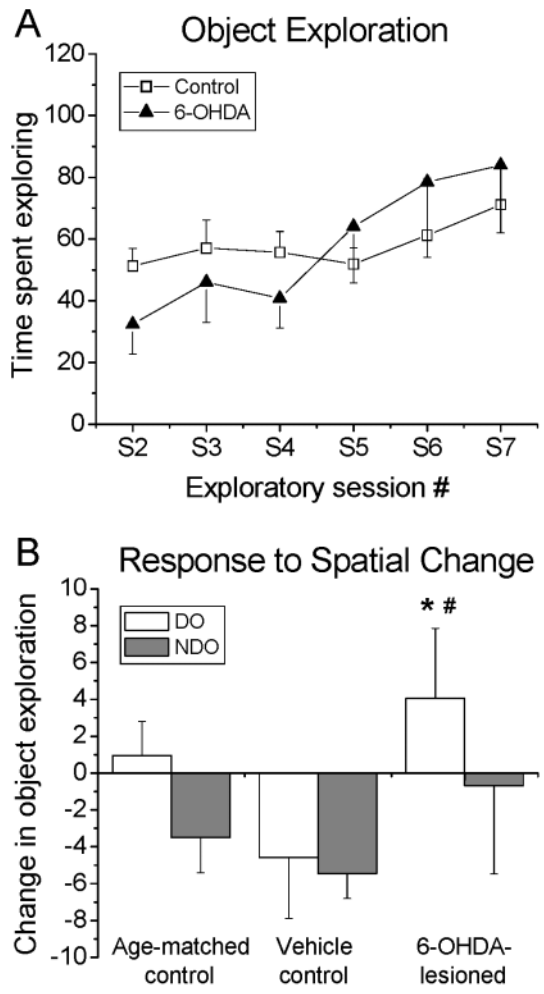

FIGURE 2 Exploratory behaviors in 6-OHDA-lesioned and vehicle-treated control mice. There was no significant difference in time spent investigating the objects in the OFOR test between the groups (**A**), although increased exploration in neurotoxin-lesioned animals in sessions 5 through 7 suggest overall increased interest in the objects. (**B**) 6-OHDA-lesioned mice increased their exploration of the displaced objects (DO) significantly compared to both vehicle and age-matched controls (*p = 0.028, ANOVA main effect) and particularly compared to vehicle control ($^{\#}p$ = 0.008, Fisher's *post-hoc* test). Vehicle-injected animals showed decreased investigation of all objects after displacement. Age-matched BALB/cByJ mice, in contrast, performed the task normally, yet still showed lower responses to the DO then 6-OHDA-lesioned mice. There was no difference in exploration of non-displaced objects (NDO) between the groups. Values represent means ± SE.

somatosensory cortex but increases in the width of the frontal cortex (Table I). Nevertheless, the increases in FC width were significant only for layer IV (p = 0.03). The decreases in the somatosensory cortical areas were consistent throughout (Table I), but displayed an anterior-posterior gradient. Separate analysis of ASSC (cortical whisker representation, Woolsey and Van der Loos, 1970) yielded no significant changes. Layer IV of BFC (encompassing the PMBS) was significantly decreased (p = 0.04) (Table I). PSSC, encompassing posterior somatosensory cortex and representations of the torso and hind-limb areas, showed decreased width of layer VI (p = 0.05) and reduced overall width (p = 0.01) (Table I). While these changes are individually small, their pervasiveness suggests a substantial morphogenetic reorganization in the cortex.

Behavioral Analysis

A. Neurological Test Battery

There were no significant differences in the placing or righting reflex, grip strength as well as beam crossing time and beam scores between 6-OHDA and vehicle-treated mice. This indicates that basic sensory-motor functions of the mice were unaffected by the lesion and supports the cortical specificity of the DA depletion.

B. OFOR

There were no differences in locomotor activity or rearing frequency between groups. Although statistically not significant, exploratory activity was initially slightly lower in 6-OHDA-lesioned mice but increased more steeply in sessions 5 and 6 when the object re-arrangement took place (FIG. 2A). The difference in overall exploratory behavior is consistent with significant difference between 6-OHDA-treated compared to vehicle control or age-matched control mice in response to the displaced object (FIG. 2B). In contrast, there were no significant differences between the groups in their responses to the novel object (data not shown).

Microarray Findings

To identify possible molecular bases for these structural and behavioral abnormalities, we analyzed transcriptional responses in the cerebral cor-

Table I Morphometrical assessments for cortical areas after 6-OHDA treatment

Cortical Layer	Group	Frontal Cortex	Somatosensory Cortex		
		FC	ASSC	BFC PMBS	PSSC
Total Cortex	Control	1102 ± 40	1094 ± 28.7	1134 ± 11	915 ± 24.6
	6-OHDA	1192 ± 13.5	1051 ± 31	1099 ± 27.2	**780 ± 46.6****
Layer II/III	Control	188 ± 12.2	217 ± 8.1	210 ± 6	187 ± 11.8
	6-OHDA	216 ± 10.7	204 ± 6.5	210 ± 9.6	163 ± 7.3
Layer IV	Control	152 ± 5.6	154 ± 6.7	177 ± 4.2	141 ± 6.8
	6-OHDA	**170 ± 5.4***	159 ± 6.5	**163 ± 5.6***	121 ± 7.5
Layer V	Control	316 ± 11.5	290 ± 10	334 ± 7.8	267 ± 10
	6-OHDA	324 ± 10.3	291 ± 8.2	310 ± 7.2	235 ± 20.8
Layer VI	Control	338 ± 11.6	335 ± 9.6	334 ± 8.7	236 ± 11.8
	6-OHDA	364 ± 7.3	313 ± 12.2	332 ± 11.8	**189 ± 22.6***

Cortical and layer widths were measured in μm. Data are expressed as means ± SE. * $p \leq 0.05$, **$p \leq 0.01$ in comparison to control mice. Bold print highlights values that showed significant differences ($p \leq 0.05$) between control and 6-OHDA-lesioned mice. Note that trends towards significant width differences are also apparent in layer IV of PSSC ($p = 0.08$) and layer VI of FC ($p = 0.09$). Neurotoxic lesions caused increases in the width of layer IV in the FC, but decreases in the BFC area of somatosensory cortex. 6-OHDA injections induced reduction in the width of layer VI in PSSC, which is also reflected in the decrease of total cortical width in this area.

Table II Biological process categories overrepresented by significantly changed genes

Categories	EASE Score
Up-regulated	
Cytoskeletion organization (9/98; 9.2%)	0.0161
Proteolysis (10/120; 8.3%)	0.0201
Small GTPase-mediated signal transduction (6/71; 8.4%)	0.0434
Down-regulated	
Translation/Protein synthesis (45/310; 14.5%)	0.0102
Regulation of transcription (17/191; 8.9%)	0.0120
Protein folding (9/140; 6.4%)	0.0257
Ion transport (14/182; 7.7%)	0.0470
Lipid transport (3/65; 4.6%)	0.0487

Biological process categories significantly overrepresented ($p < 0.05$; EASE score) are shown. Significant functional categories are those with a higher ratio of identified genes to all genes tested on the array for associations with that category, relative to the ratio of total identified genes in the study to all genes tested on the array for associations with all categories. After each category description (in parentheses) is the ratio of associations for that category and the percentage represented by that ratio. EASE, modified Fisher's exact test p value. The complete list of significantly changed genes is given in Supplementary Table I.

tex after neonatal 6-OHDA treatment. We elected to assay gene expression on PND 7 because the first postnatal week is a highly dynamic period, during which time most of the mature cortical architecture and connectivity becomes specified in rodents (for review see: Berger-Sweeney and Hohmann, 1997; Dikranian *et al.*, 2001; Hohmann, 2003). Towards that end, 6-OHDA-lesioned animals were compared to vehicle-treated mice by using microarray technology and several data mining tools. Our analyses revealed that 866 out of 16,896 transcripts were differently regulated in the cortices of 6-OHDA-treated and control mice ($p < 0.05$). To concentrate on changes that can be interpreted in a context of gene function, we included only genes classified using the on-line gene classification tool DAVID 2.0 (http://david.niaid.nih.gov/David) in further analyses and excluded all undefined ESTs. With these exclusion criteria, only 227 of the 866 transcripts were left for further analyses. We applied hierarchical cluster analysis to profile these transcripts based on similarity between their expression patterns (FIG. 3). Two differential expression profiles were obtained showing that 100 genes were significantly up-regulated (FIG. 3, cluster A) whereas 127 genes were significantly down-regulated (FIG. 3, cluster B) after DA depletion. Using DAVID 2.0 classification tool, we grouped these genes according to functional classes. The up-regulated transcripts belong to several classes including those that play a role in differentiation and synaptogenesis, cytoskeletal development, neuronal apoptosis, regulation of transcription, translation/protein synthesis, signal transduction, intracellular transport, cell adhesion, DNA damage and stress response. The down-regulated transcripts also fall within similar classifications. A full list of differentially expressed genes with their functional classification is available as supplemental material (Supplementary Table I).

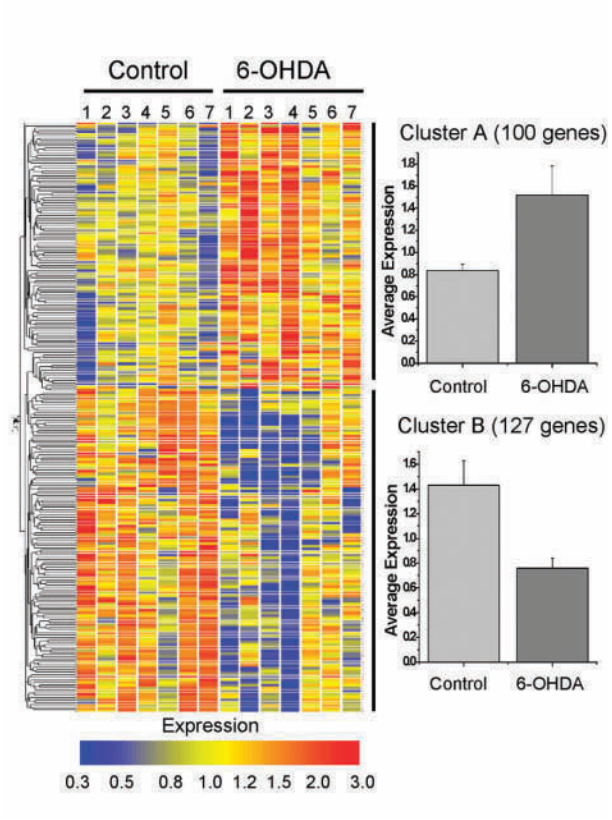

FIGURE 3 Hierarchical cluster analysis of gene expression profiles in the cortex of vehicle and 6-OHDA-treated mice. 227 genes whose transcript levels were affected by DA depletion were selected based on criteria described in the text. These genes were grouped into two clusters (**A, B**) according to their patterns of expression. The gene expression levels were quantified after median normalization and logarithmic transformation. For each gene, the expression in the control and 6-OHDA-treated groups is shown individually for each animal and represented by a color according to color scale at the bottom. Each row shows changes in the expression of a single gene in individual animals in both control and 6-OHDA-treated groups, where each column represents the variation in the expression of the genes within a particular animal. The dendrogram on the left side of the cluster shows the statistical relatedness of the genes in the cluster, with shorter branches representing closer relations between genes. The graphs on the right show the average expression profiles for the genes in the corresponding cluster.

Using EASE analysis, we identified biological process categories that showed a disproportionally high number of co-regulated genes (significant overrepresentation of changed genes in those categories). The Gene Ontology Biological Process categories in which significantly changed genes were overrepresented by EASE score ($p < 0.05$) are shown in Table II. For up-regulated genes, a major difference was seen in cytoskeleton organization category that included several individual tubulin subunits. In addition, proteolysis and small GTPase-mediated signal transduction were overrepresented in up-regulated genes. Although their categories were not overrepresented, several up-regulated genes, including transforming growth factor α, bone morphogenetic protein 8b and glia

maturation factor β reflected injury response and glial activation process (Supplementary Table I). Translation/protein synthesis and regulation of transcription were two largest categories of down-regulated genes. In addition, protein folding as well as ion and lipid transport were overrepresented in down-regulated genes.

We decided to focus the present report on some genes that are involved in the regulation of differentiation and synaptogenesis, formation of the cytoskeleton and neuronal apoptosis because of their well established role in cortical development. The list of selected transcripts significantly changed in these functional classes is provided in Table III. Genes that code for proteins involved in neuronal differentiation and synaptogenesis include DA depletion-induced increases in Sema3A transcript levels. Expression of several genes whose products participate in cytoskeletal formation was also altered after the 6-OHDA injections. For example, RhoD, which regulates microtubule dynamics (Govek *et al.*, 2005), and tubulin β5 microtubule subunit were up-regulated. In contrast, down-regulated were the chaperonins, CCTε and CCTζ, which are involved in folding of the cytoskeletal proteins, actin and tubulin (Valpuesta *et al.*, 2002). Genes such as c-Jun and MEF2D that support neuronal survival during development were also down-regulated in the DA depleted cortex. On the other hand, the expression of GAPDH, which is involved in neuronal apoptosis (Chuang *et al.*, 2005) was significantly increased.

Real-time RT-PCR

We used quantitative RT-PCR to confirm the changes in transcripts selected based on their involvement in differentiation and synaptogenesis (Sema3A), in cytoskeleton formation (tubulin β5, CCTε, CCTζ and RhoD), or in neuronal survival

Table III Partial list of 6-OHDA-regulated genes

GenBank#	Gene Name	Symbol	Control	6-OHDA	*p* values
			Means ± SE	Means ± SE	
		Differentiation / Synaptogenesis			
Up-regulated					
BQ551360	Semaphorin 3A	Sema3A	0.76 ± 0.11	1.29 ± 0.17	0.031
		Cytoskeleton			
Up-regulated					
BG084568	Tubulin cofactor a	TBCα	0.66 ± 0.08	1.29 ± 0.10	0.001
BG087420	Tubulin, beta 5	TUBβ5	0.88 ± 0.08	1.34 ± 0.17	0.028
BQ551468	Tubulin, delta 1	TUBδ1	0.88 ± 0.06	1.51 ± 0.25	0.024
AU041357	Ras homolog D	RhoD	0.91 ± 0.08	1.29 ± 0.1 3	0.036
Down-regulated					
BG064770	Chaperonin subunit 5 (epsilon)	CCTε	1.36 ± 0.17	0.72 ± 0.10	0.015
BQ550999	Chaperonin subunit 6a (zeta)	CCTζ	1.65 ± 0.42	0.58 ± 0.19	0.007
		Apoptosis			
Up-regulated					
BC064681	Glyceraldehyde-3-phosphate dehydrogenase	GAPDH	0.78 ± 0.38	1.91 ± 0.37	0.015
Down-regulated					
BG080846	Jun oncogene	c-Jun	1.33 ± 014	0.82 ± 0.13	0.019
BG080755	Myocyte enhancer factor 2D	MEF2D	1.48 ± 0.22	0.92 ± 0.15	0.040

and apoptosis (c-Jun, MEF2D, GAPDH). As shown in FIG. 4, consistent with microarray findings, significant changes were observed in the same direction for all genes studied. Specifically, DA depletion caused an induction (+45%) of Sema3A mRNA (FIG. 4A). Similarly, GAPDH (+22%) and tubulin β5 (+34%) mRNA levels were increased after 6-OHDA treatment (FIG. 4B, 4C). Expression of RhoD mRNA was also up-regulated (+20%) (FIG. 4D). In contrast, c-Jun mRNA was decreased (-39%) (FIG. 5E). In addition, there was a small, but significant down-regulation in the expression of CCTζ (-14%) and CCTε (-16%) mRNAs (FIG. 4F, 4G). Similarly, DA depletion caused decreases in MEF2D (-17%) transcript levels in the cortex of 6-OHDA-treated animals (FIG. 4H).

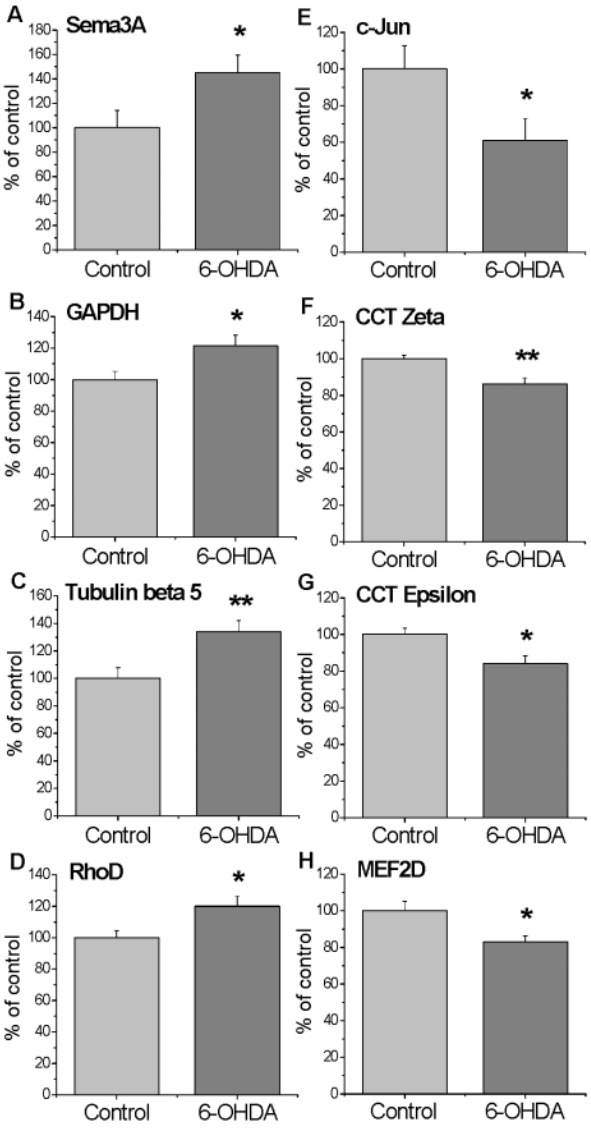

FIGURE 4 Quantitative RT-PCR analyses of some transcripts affected by DA depletion. The expression of genes, selected based on their potential involvement in neurodevelopmental processes, was confirmed by RT-PCR. For all genes examined, statistically significant changes were observed in the same direction as microarray results. The data were obtained for RNA samples isolated from 7 mice per group and determined individually. The amount of each product was normalized by 18S. Values represent means ± SE (% of respective controls). *p <0.05, **p <0.01 in comparison to control.

DISCUSSION

The first postnatal week in rodents represents the most dynamic period in cortical development when neuronal migration concludes, differentiation and synaptogenesis are initiated, and apoptosis prunes neuronal populations (Berger-Sweeney and Hohmann, 1997; Dikranian *et al.*, 2001). At this time, afferent neurotransmitter projections from brainstem and basal forebrain orchestrate cortical development by providing important growth and differentiation stimuli to neurons (Berger-Sweeney and Hohmann, 1997; Foehring and Lorenzon, 1999). Herein, we have addressed the role of the DA afferents in the regulation of cortical development by using a strategy combining histological and behavioral tests, as well as microarray technology and quantitative RT-PCR in an animal model of deficient cortical DA innervation. This strategy was designed to identify candidate genes that mediate a morphogenetic role of DA in cortical development and behavioral regulation.

In the present study, we applied 6-OHDA directly to the mesocortical DA afferents via injections into the MFB at the level of the substantia innominata/diagonal band of Broca. This empirically derived focal approach allowed us to obtain significant DA depletions in the cortex with ~10% of neurotoxin doses typically used for i.c.v. or intracisternal administration (Miller *et al.*, 1981; Raskin *et al.*, 1983; Archer *et al.*, 1988; Luthman *et al.*, 1997) while simultaneously sparing other afferent monoaminergic projections. In contrast to earlier studies (Onteniente *et al.*, 1980; Blue and Molliver, 1987; Molina-Holgado *et al.*, 1993), our 6-OHDA injection protocol did not cause decreases in cortical NE

levels nor compensatory increases in 5-HT concentrations. In addition, the appearance of non-specific lesions of surrounding tissues was eliminated and the physical health of treated animals was not affected. Thus, this approach permitted us to measure morphological, behavioral and gene expression effects derived selectively from DA depletion to the neocortex of mice.

The specificity of the DA depletion might be responsible, in part, for the more subtle behavioral deficits observed in our studies in comparison with most previously published models (Miller *et al.*, 1981; Raskin *et al.*, 1983; Archer *et al.*, 1988; Luthman *et al.*, 1997). Consistent with some other reports of more selectively neonatally 6-OHDA-lesioned mice (Joyce *et al.*, 1996; Bruno *et al.*, 1998), we did not find significant locomotor alterations in adult animals following our treatment protocol. Thus, altered gross motor performance may be related primarily to striatal DA depletions in the mature rodent brain. Moreover, i.c.v. and intracisternal 6-OHDA injections are more likely to alter 5-HT concentrations in addition to their effects on DA levels (Molina-Holgado *et al.*, 1993; Joyce *et al.*, 1996; Luthman *et al.*, 1997). Indeed, increased 5-HT sprouting and associated elevated 5-HT levels induced by neonatal 6-OHDA treatment have been implicated in the occurrence of abnormalities in skilled motor performance including tongue or limb use (Joyce *et al.*, 1996; Luthman *et al.*, 1997). The developmental timing of the lesion may also influence the behavioral outcome, because rats that received 6-OHDA injections at PND7 had substantial abnormalities whereas animals lesioned on PND0/1 showed no locomotor changes and minimal sensorimotor deficits (Neal-Beliveau and Joyce, 1999).

The significant behavioral difference in the performance of our lesioned mice occurred in the object displacement phase of the OFOR task. Lesioned mice initially showed less exploration of the objects in the task but substantially increased their exploratory behavior in later sessions likely in response to altered object placement. Neonatally 6-OHDA-treated animals showed increased exploration of the displaced objects. This part of the OFOR (S5, S6) is generally used to assess the ability to recognize spatial change and thus is commonly regarded as a spatial learning and memory task (Roullet and Lassalle, 1990; Thinus-Blanc *et al.*, 1996; Ricceri *et al.*, 1999). Increased exploration of the displaced, but not non-displaced objects by 6-OHDA-lesioned mice compared to vehicle-injected controls suggests that animals recognized the spatial change but nevertheless, showed an altered response compared to vehicle control mice. This behavior cannot be attributed to hyperemotionality to novelty, because response to the substituted object in S7 did not differ between 6-OHDA-lesioned and control mice. We suggest that increased exploration of displaced objects in 6-OHDA-treated mice may be the consequence of impaired motor inhibition following neonatal DA depletion (Sullivan and Brake, 2003) or, less likely, represent compromised working memory in the presence of intact reference and procedural memory. In other words, mice might be aware that their spatial environment has changed but do not recall how to respond to that change properly. Either interpretation would point at disrupted cortical regulation of cognitive function. Future behavioral studies will have to differentiate frontal versus parietal cortical involvement. Interestingly, our vehicle-injected control mice showed the opposite response to 6-OHDA-lesioned mice. Vehicle-injected mice reduced all exploration after object displacement. We have seen similar behavior in response to neonatal stress in another study in our lab (C.F. Hohmann, unpublished observations) and hypothesize that this behavior results from the stress associated with the surgical procedure. It is remarkable that although 6-OHDA-depleted mice have sustained the same surgical procedure, the neonatal cortical DA depletion has evidently reversed this effect.

In addition to the behavioral changes observed in these animals, histological analysis revealed significant alterations in cortical width and laminar cytoarchitecture following 6-OHDA treatment that varied between cortical areas and layers. Lesion effects extended from the frontal cortex to posterior somatosensory cortex. While these results appear to run counter to the common perception that the DA innervation in rodents is restricted to frontal and limbic cortical structures, they are consistent with data from previous reports (Descarries *et al.*, 1987; Berger *et al.*, 1991) that provided evidence for heterogeneous cortical DA projections in the rodent brain. Specifically, these studies showed

DA innervation to parietal, temporal and occipital cortices, in addition to frontal cortical areas, with a rostrocaudal gradient of decreasing density from the prefrontal to occipital cortex (Descarries *et al.*, 1987; Berger *et al.*, 1991). It is to be noted that cytoarchitectonic changes caused by DA depletion were differentially expressed in frontal and parietal cortical areas, suggesting that these regions are affected in a manner that may reflect their functional differences. There were increases in the width of the frontal cortex but decreases in somatosensory cortical areas. Layers IV and VI involved in sensorimotor processing were most affected. Such layer specificity suggests that these effects result from cortical, but not striatal DA depletion. Layer IV is the recipient layer of primary sensory input from the thalamus, and layer VI predominantly provides feedback projections to the same thalamic nuclei. Layer V, involved with striatal and downstream motor projections, is not significantly altered in any cortical area we assessed. Our observations are entirely consistent with those of previous reports of decreases in cortical width, reductions in synapses, spines, and dendritic branching as a consequence of less selective DA depletion (Kalsbeek *et al.*, 1987; 1989b) as well as with recent study of selective DA depletions to fronto-limbic cortical areas (Sherren and Pappas, 2005). Thus, when taken together, accumulated evidence suggests that DA deafferentation in the developing cortex might impact neuronal differentiation and connectivity. This likely would occur through dysregulation of transcriptional programs that are important to the normal development of cortical cytoarchitecture.

In order to test this idea, we opted to assay gene expression in corresponding regions of the cortex in our 6-OHDA-treated mice. We chose PND7 for this analysis since the first postnatal week is a highly dynamic period during which most of the mature cortical architecture and connectivity becomes specified (Berger-Sweeney and Hohmann, 1997; Dikranian *et al.*, 2001; Hohmann, 2003). We are able to show here that 6-OHDA lesions are selectively associated with significantly altered expression of genes implicated in neuronal differentiation and target finding along with changes in the transcription of genes involved in other cellular pathways. Biological process categories, identified statistically (EASE program), revealed a significant overrepresentation of genes involved in the regulation of transcription, translation/protein synthesis and protein folding among down-regulated categories. This agrees with previous studies showing that afferents control cortical ontogeny via receptor-mediated post-synaptic activity able to regulate transcriptional programs which orchestrate protein synthesis, mitochondrial function and suppress apoptosis (Sherrard and Bower, 1998; Gu, 2002; Hohmann, 2003). Therefore, depletion of DA afferents appears to have resulted in significant down-regulation in transcription, translation and protein synthesis in cortical cells. The significant overrepresentation of genes involved in proteolysis among up-regulated categories may reflect the increased degradation of misfolded proteins and is consistent with the observed down-regulation of mRNAs involved in protein folding. Increase in transforming growth factor α, bone morphogenetic protein 8b and glia maturation factor β, transcripts that may be involved in injury response and glial activation, is consistent with the hypothesis of decreased trophic support from depleted DA afferents that may cause cellular damage (Sherrard and Bower, 1998). Our data are in agreement with results of previous studies that used microarray analyses after 6-OHDA-induced lesions showing reduction in the expression of genes involved in the regulation of transcription (Napolitano *et al.*, 2002) and increased expression of transcripts whose products play a role in cellular stress and unfolded protein response (Holtz and O'Malley, 2003).

Several gene expression changes in the categories of differentiation/synaptogenesis, particularly in regards to cytoskeleton formation, growth cone guidance and apoptosis were further investigated by quantitative RT-PCR because of their significance to our morphologic observations. In what follows, we discuss the possible relevance of some of these changes to the neuropathological effects observed in the cortex of the neurotoxin-treated mice.

Perhaps, the most intriguing finding was that DA depletion caused increase in the expression of Sema3A in the cortex at PND7. Sema3A belongs to a large semaphorin family whose members play a critical role in axonal and dendritic guidance in the developing nervous system (Goshima *et al.*, 2002; Kruger *et al.*, 2005). In the cortex, Sema3A provides repulsive signals to axonal growth cones (Goshima

et al., 2002) and induces rapid actin depolymerization followed by growth cone collapse (Fournier *et al.*, 2000). In addition, Sema3A accelerates endocytosis and promotes actin-cytoskeletal reorganization (Fournier *et al.*, 2000; Dent *et al.*, 2004). Thus, up-regulation of Sema3A after 6-OHDA treatment may serve to inhibit axonal growth and impair the ability to establish timely synaptic connections between neurons in the developing cortex. Because high concentrations of Sema3A can also cause severe axonal damage and neuronal apoptosis in the absence of other apoptotic triggers (Shirvan *et al.*, 1999), increase in Sema3A expression might be involved in neuronal loss following neonatal DA depletion. In agreement with the present findings, recent microarray study of developing striatum from rats treated with DA toxin methamphetamine *in utero* (Noailles *et al.*, 2003) found changes in the expression of genes that participate in neuronal migration and synaptic formation, including an increase in Sema3A levels. It is of interest that elevated Sema3A protein concentrations may contribute to the synaptic pathology in schizophrenia (Eastwood *et al.*, 2003).

The argument that the observed transcriptional effects might underlie the changes in cortical width of 6-OHDA-treated mice is supported by the findings of up-regulation of the neural-specific, tubulin β5 isoform. Increased levels of β-tubulin are toxic to cells because high concentration of the protein interferes with normal microtubule assembly by forming abnormal β-tubulin-enriched tubulin heterodimers followed by rapid depolymerization of microtubules that affect cell viability (Burke *et al.*, 1989; Weinstein and Solomon, 1990). This idea is underlined by the observation that the increase in tubulin β5 expression is accompanied by down-regulation of the chaperonin CCT subunits, CCTε and CCTζ, which are involved in the correct folding of tubulin and actin monomers and in the assembly of functional heterodimers (Valpuesta *et al.*, 2002). Thus, DA depletion-induced decreases in the expression of CCTε and CCTζ can cause the formation of misfolded tubulin followed by depolymerization of microtubules which are cytotoxic (Burke *et al.*, 1989; Weinstein and Solomon, 1990). This discussion is further supported by reports that mutations in CCT subunits can cause major cytoskeletal defects by failing to assemble functional microtubules and normal actin structures (Chen *et al.*, 1994; Vinh and Drubin, 1994). Misfolded cytoskeletal actin may also result in decreased motility of dendritic and axonal extensions (Bradke and Dotti, 1999; Jan and Jan, 2003) which would negatively influence the formation of synaptic connections and cortical width. This argument is also relevant to the observations of 6-OHDA-induced increased expression of RhoD GTPase because members of Rho GTPases regulate actin cytoskeletal reorganization and play a role in microtubule orientation and stabilization (Govek *et al.*, 2005). The importance of actin and microtubule cytoskeleton in axonal and dendritic functions suggests that Rho GTPases are critical to their formation and maintenance (Govek *et al.*, 2005). Indeed, Rho GTPase activation prevents axon formation (Arakawa *et al.*, 2003), dramatically reduces dendritic growth (Li *et al.*, 2000; Pilpel and Segal, 2004) and causes decreases in the number of dendritic spines (Wong *et al.*, 2000). The observations of decreased dendritic length in the developing cortex after selective neonatal DA lesions (Sherren and Pappas, 2005) support the contention that the presently observed up-regulation of RhoD might be one of the pathogenic factors.

Taken together, the changes in selected genes appear to reflect reduced synaptogenesis and defects in cytoskeleton formation in developing neurons in parallel with elevated apoptosis in the cortex. Thus, the DA-dependent transcripts identified here likely represent good candidates for factors that impact on cortical development. These alterations apparently precede measurable morphological abnormalities and behavioral impairments in adult performance.

In summary, this paper has introduced a new model to test the hypothesis that DA serves as a morphogen in the ontogeny of fronto-parietal cortex. The histological changes obtained here are consistent with previous observations following neonatal 6-OHDA lesions. The present findings support the idea that DA afferents regulate gene expression programs that orchestrate morphogenesis and promote neuronal survival in the developing cortex. Indeed, dysregulation of these pathways in the cortex, following neonatal DA depletion, is consistent with both the morphological and behavioral observations in our and previous models (Kalsbeek *et al.*, 1989b; Sherren and

Pappas, 2005). Our data suggest that impaired dendritic and axonal development, as consequence of disruptions of the cytoskeleton and growth cone guidance, might have led to changes in cortical architecture and compromised connectivity within the cortex as well as between cortical and subcortical regions with resulting behavioral abnormalities in rodents. Future studies will have to determine to what extent the affected genes are unique to the morphogenetic effects of DA or shared with other modulatory mechanisms. Finally, our results are of clinical relevance to the elucidation of molecular and cellular programs involved in neurodevelopmental disorders such as schizophrenia (Harrison and Weinberger, 2005), ADHD (Shastry, 2004) and Rett syndrome (Johnston *et al.*, 1995), all three of which appear to show dysregulations of cortical DA innervation.

Acknowledgements

This research was supported by the Intramural Research Programs of the National Institute on Drug Abuse (to I.N.K., E.S.B., B.L. and J.L.C.) and National Institute of Aging (to K.G.B.) of the NIH/DHHS, as well as by grants PO1HD24448, SO6-GM051971-9 and 1G12RR17581 (to C.F.H.).

References

Arakawa Y, H Bito, T Furuyashiki, T Tsuji, S Takemoto-Kimura, K Kimura, K Nozaki, N Hashimoto and S Narumiya (2003) Control of axon elongation via an SDF-1alpha/Rho/mDia pathway in cultured cerebellar granule neurons. *J. Cell Biol.* **161**, 381-391.

Archer T, W Danysz, A Fredriksson, G Jonsson, J Luthman, E Sundstrom and A Teiling (1988) Neonatal 6-hydroxydopamine-induced dopamine depletions: motor activity and performance in maze learning. *Pharmacol. Biochem. Behav.* **31**, 357-364.

Benes FM, JB Taylor and MC Cunningham (2000) Convergence and plasticity of monoaminergic systems in the medial prefrontal cortex during the postnatal period: implications for the development of psychopathology. *Cereb. Cortex* **10**, 1014-1027.

Berger B, P Gaspar and C Verney (1991) Dopaminergic innervation of the cerebral cortex: unexpected differences between rodents and primates. *Trends Neurosci.* **14**, 21-27.

Berger-Sweeney J and CF Hohmann (1997) Behavioral consequences of abnormal cortical development: insights into developmental disabilities. *Behav. Brain Res.* **86**, 121-142.

Berger-Sweeney J, M Libbey, J Arters, M Junagadhwalla and CF Hohmann (1998) Neonatal monoaminergic depletion in mice (*Mus. musculus*) improves performance of a novel odor discrimination task. *Behav. Neurosci.* **112**, 1318-1326.

Blue ME and ME Molliver (1987) 6-Hydroxydopamine induces serotonergic axon sprouting in cerebral cortex of newborn rat. *Brain Res.* **429**, 255-269.

Blue ME, RS Erzurumlu and S Jhaveri (1991) A comparison of pattern formation by thalamocortical and serotonergic afferents in the rat barrel field cortex. *Cereb. Cortex* **1**, 380-389.

Boylan CB, CA Bennett-Clarke, RS Crissman, RD Mooney and RW Rhoades (2000) Clorgyline treatment elevates cortical serotonin and temporarily disrupts the vibrissae-related pattern in rat somatosensory cortex. *J. Comp. Neurol.* **427**, 139-149.

Bradke F and CG Dotti (1999) The role of local actin instability in axon formation. *Science* **283**, 1931-1934.

Brazma A, P Hingamp, J Quackenbush, G Sherlock, P Spellman, C Stoeckert, J Aach, W Ansorge, CA Ball, HC Causton, T Gaasterland, P Glenisson, FC Holstege, IF Kim, V Markowitz, JC Matese, H Parkinson, A Robinson, U Sarkans, S Schulze-Kremer, J Stewart, R Taylor, J Vilo and M Vingron (2001) Minimum information about a microarray experiment (MIAME)-toward standards for microarray data. *Nat. Genet.* **29**, 365-371.

Breese GR, DJ Knapp, HE Criswell, SS Moy, ST Papadeas and BL Blake (2005) The neonate-6-hydroxydopamine-lesioned rat: a model for clinical neuroscience and neurobiological principles. *Brain Res. Brain Res. Rev.* **48**, 57-73.

Bruno JP, MI Sandstrom, H Arnold and CL Nelson (1998) Age-dependent neurobehavioral plasticity following forebrain dopamine depletions. *Dev. Neurosci.* **20**, 164-179.

Burke D, P Gasdaska and L Hartwell (1989) Dominant effects of tubulin overexpression in *Saccharomyces cerevisiae. Mol. Cell. Biol.* **9**, 1049-1059.

Chen X, DS Sullivan and TC Huffaker (1994) Two yeast genes with similarity to TCP-1 are required for microtubule and actin function *in vivo. Proc. Natl. Acad. Sci. USA* **91**, 9111-9115.

Chuang DM, C Hough and VV Senatorov (2005) Glyceraldehyde-3-phosphate dehydrogenase, apoptosis, and neurodegenerative diseases. *Annu. Rev. Pharmacol. Toxicol.* **45**, 269-290.

Cohen-Cory S (2002) The developing synapse: construction and modulation of synaptic structures and circuits. *Science* **298**, 770-776.

Dennis G Jr, BT Sherman, DA Hosack, J Yang, W Gao, HC Lane and RA Lempicki (2003) DAVID: Database for Annotation, Visualization, and Integrated Discovery. *Genome Biol.* **4**, P3.

Dent EW, AM Barnes, F Tang and K Kalil (2004) Netrin-1 and semaphorin 3A promote or inhibit cortical axon branching, respectively, by reorganization of the cytoskeleton. *J. Neurosci.* **24**, 3002-3012.

Descarries L, B Lemay, G Doucet and B Berger (1987) Regional and laminar density of the dopamine innervation in adult rat cerebral cortex. *Neuroscience* **21**, 807-824.

Dikranian K, MJ Ishimaru, T Tenkova, J Labruyere, YQ Qin, C Ikonomidou and JW Olney (2001) Apoptosis in the *in vivo* mammalian forebrain. *Neurobiol. Dis.* **8**, 359-379.

Durston S (2003) A review of the biological bases of ADHD:

what have we learned from imaging studies? *Ment. Retard. Dev. Disabil. Res. Rev.* **9**, 184-195.

Eastwood SL, AJ Law, IP Everall and PJ Harrison (2003) The axonal chemorepellant semaphorin 3A is increased in the cerebellum in schizophrenia and may contribute to its synaptic pathology. *Mol. Psychiatry* **8**, 148-155.

Foehring RC and NM Lorenzon (1999) Neuromodulation, development and synaptic plasticity. *Can. J. Exp. Psychol.* **53**, 45-61.

Fournier AE, F Nakamura, S Kawamoto, Y Goshima, RG Kalb and SM Strittmatter (2000) Semaphorin3A enhances endocytosis at sites of receptor-F-actin colocalization during growth cone collapse. *J. Cell Biol.* **149**, 411-422.

Goshima Y, T Ito, Y Sasaki and F Nakamura (2002) Semaphorins as signals for cell repulsion and invasion. *J. Clin. Invest.* **109**, 993-998.

Govek EE, SE Newey and L Van Aelst (2005) The role of the Rho GTPases in neuronal development. *Genes Dev.* **19**, 1-49.

Gu Q (2002) Neuromodulatory transmitter systems in cortex and their role in cortical plasticity. *Neuroscience* **111**, 815-835.

Guillemot F, Z Molnar, V Tarabykin and A Stoykova (2006) Molecular mechanisms of cortical differentiation. *Eur. J. Neurosci.* **23**, 857-868.

Harrison PJ and DR Weinberger (2005) Schizophrenia genes, gene expression and neuropathology: on the matter of their convergence. *Mol. Psychiatr.* **10**, 40-68.

Hohmann CF (2003) A morphogenetic role for acetylcholine in mouse cerebral neocortex. *Neurosci. Biobehav. Rev.* **27**, 351-363.

Hohmann CF and J Berger-Sweeney (1998) Sexually dimorphic responses to neonatal basal forebrain lesions in mice: II Quantitative assessments of cortical morphology. *J. Neurobiol.* **5**, 401-425.

Hohmann CF, AR Brooks and JT Coyle (1988) Neonatal lesions of the basal forebrain cholinergic neurons result in abnormal cortical development. *Brain Res. Dev. Brain Res.* **43**, 253-264.

Hohmann CF, C Richardson, E Pitts and J Bareger-Sweeney (2000) Neonatal 5,7-DHT lesions cause sex specific changes in mouse cortical morphogenesis. *Neural Plast.* **7**, 313-332.

Holtz WA and KL O'Malley (2003) Parkinsonian mimetics induce aspects of unfolded protein response in death of dopaminergic neurons. *J. Biol. Chem.* **278**, 19367-19377.

Hosack DA, G Dennis Jr, BT Sherman, HC Lane and RA Lempicki (2003) Identifying biological themes within lists of genes with EASE. *Genome Biol.* **4**, R70.

Jan YN and LY Jan (2003) The control of dendrite development. *Neuron* **40**, 229-242.

Johnston MV, C Hohmann and ME Blue (1995) Neurobiology of Rett Syndrome. *Neuropediatrics* **26**, 119-122.

Johnston MV, OH Jeon, J Pevsner, ME Blue and S Naidu (2001) Neurobiology of Rett Syndrome: a genetic disorder of synapse development. *Brain Dev.* **23**, 206-213.

Joyce JN, PA Frohna and BS Neal-Beliveau (1996) Functional and molecular differentiation of the dopamine system induced by neonatal denervation. *Neurosci. Biobehav. Rev.* **20**, 453-486.

Kalsbeek A, RM Buijs, MA Hofman, MA Matthijssen, CW Pool and HB Uylings (1987) Effects of neonatal thermal lesioning of the mesocortical dopaminergic projection on the development of the rat prefrontal cortex. *Brain Res.* **429**, 123-132.

Kalsbeek A, JP de Bruin, MA Matthijssen and HB Uylings (1989a) Ontogeny of open field activity in rats after neonatal lesioning of the mesocortical dopaminergic projection. *Behav. Brain Res.* **32**, 115-127.

Kalsbeek A, MA Matthijssen and HB Uylings (1989b) Morphometric analysis of prefrontal cortical development following neonatal lesioning of the dopaminergic mesocortical projection. *Exp. Brain Res.* **78**, 279-289.

Krasnova IN, B Ladenheim, S Jayanthi, J Oyler, TH Moran, MA Huestis and JL Cadet (2001) Amphetamine-induced toxicity in dopamine terminals in CD-1 and C57BL/6J mice: complex roles for oxygen-based species and temperature regulation. *Neuroscience* **107**, 265-274.

Krasnova IN, MT McCoy, B Ladenheim and JL Cadet (2002) cDNA array analysis of gene expression profiles in the striata of wild-type and Cu/Zn superoxide dismutase transgenic mice treated with neurotoxic doses of amphetamine. *FASEB J.* **16**, 1379-1388.

Krasnova IN, B Ladenheim and JL Cadet (2005) Amphetamine induces apoptosis of medium spiny striatal projection neurons via the mitochondria-dependent pathway. *FASEB J.* **19**, 851-853.

Kruger RP, J Aurandt and KL Guan (2005) Semaphorins command cells to move. *Nat. Rev. Mol. Cell. Biol.* **6**, 789-800.

Li Z, L Van Aelst and HT Cline (2000) Rho GTPases regulate distinct aspects of dendritic arbor growth in *Xenopus* central neurons *in vivo*. *Nat. Neurosci.* **3**, 217-225.

Luthman J, E Brodin, E Sundstrom and B Wiehager (1990) Studies on brain monoamine and neuropeptide systems after neonatal intracerebroventricular 6-hydroxydopamine treatment. *Int. J. Dev. Neurosci.* **8**, 549-560.

Luthman J, M Bassen, A Fredriksson and T Archer (1997) Functional changes induced by neonatal dopamine treatment: effects of dose levels on behavioral parameters. *Behav. Brain Res.* **82**, 213-221.

Mick E, J Biederman, SV Faraone, J Sayer and S Kleinman (2002) Case-control study of attention-deficit hyperactivity disorder and maternal smoking, alcohol use, and drug use during pregnancy. *J. Am. Acad. Child Adolesc. Psychiatry* **41**, 378-385.

Miller FE, TG Heffner, C Kotake and LS Seiden (1981) Magnitude and duration of hyperactivity following neonatal 6-hydroxydopamine is related to the extent of brain dopamine depletion. *Brain Res.* **229**, 123-132.

Molina-Holgado E, KM Dewar, L Grondin, NM van Gelder and TA Reader (1993) Amino acid levels and gamma-aminobutyric acidA receptors in rat neostriatum, cortex, and thalamus after neonatal 6-hydroxydopamine lesion. *J. Neurochem.* **60**, 936-945.

Napolitano M, D Centonze, A Calce, B Picconi, S Spiezia, A Gulino, G Bernardi and P Calabresi (2002) Experimental parkinsonism modulates multiple genes involved in the transduction of dopaminergic signals in the striatum. *Neurobiol. Dis.* **10**, 387-395.

Neal-Beliveau BS and JN Joyce (1999) Timing: a critical determinant of the functional consequences of neonatal 6-OHDA lesions. *Neurotox. Teratol.* **21**, 129-140.

Noailles PA, KG Becker, WH Wood 3rd, D Teichberg and JL Cadet (2003) Methamphetamine-induced gene expression profiles in the striatum of male rat pups exposed to the drug *in utero*. *Brain Res. Dev. Brain Res.* **147**, 153-162.

Onteniente B, N Konig, J Sievers, S Jenner, HP Klemm and R Marty (1980) Structural and biochemical changes in rat cerebral cortex after neonatal 6-hydroxdopamine administration. *Anat. Embryol.* **159**, 245-255.

Pappas BA, SJ Murtha, GA Park, KT Condon, RM Szirtes, SI Laventure and A Ally (1992) Neonatal brain dopamine depletion and the cortical and behavioral consequences of enriched postweaning environment. *Pharmacol. Biochem. Behav.* **42**, 741-748.

Pilpel Y and M Segal (2004) Activation of PKC induces rapid morphological plasticity in dendrites of hippocampal neurons via Rac and Rho-dependent mechanisms. *Eur. J. Neurosci.* **19**, 3151-3164.

Poucet B (1989) Object exploration, habituation and response to spatial change in rats following septal or medial frontal cortical damage. *Behav. Neurosci.* **103**, 1009-1016.

Price DJ, H Kennedy, C Dehay, L Zhou, M Mercier, Y Jossin, AM Goffinet, F Tissir, D Blakey and Z Molnar (2006) The development of cortical connections. *Eur. J. Neurosci.* **23**, 910-920.

Raedler TJ, MB Knable and DR Weinberger (1998) Schizophrenia as a developmental disorder of the cerebral cortex. *Curr. Opin. Neurobiol.* **8**, 157-161.

Raskin LA, BA Shaywitz, GM Anderson, DJ Cohen, MH Teicher and J Linakis (1983) Differential effects of selective dopamine, norepinephrine or catecholamine depletion on activity and learning in the developing rat. *Pharmacol. Biochem. Behav.* **19**, 743-749.

Ricceri L, A Usiello, A Valanzano, G Calamandrei, K Frick and J Berger-Sweeney (1999) Neonatal ^{192}IgG-saporin lesions of basal forebrain cholinergic neurons selectively impair response to spatial novelty in adult rats. *Behav. Neurosci.* **113**, 1204-1215.

Rice D and S Barone Jr (2000) Critical periods of vulnerability for the developing nervous system: evidence from humans and animal models. *Environ. Health Perspect.* **108** Suppl. 3, 511-533.

Roth RM and AJ Saykin (2004) Executive dysfunction in attention-deficit/hyperactivity disorder: cognitive and neuroimaging findings. *Psychiatr. Clin. North Am.* **27**, 83-96, ix.

Roullet P and JM Lassalle (1990) Genetic variation, hippocampal mossy fiber distribution, novelty reaction and spatial representation in mice. *Behav. Brain Res.* **41**, 61-70.

Shastry BS (2004) Molecular genetics of attention-deficit hyperactivity disorder (ADHD): and update. *Neurochem. Int.* **44**, 469-474.

Shenton ME, CC Dickey, M Frumin and RW McCarley (2001) A review of MRI findings in schizophrenia. *Schizophr. Res.* **49**, 1-52.

Sherrard RM and AJ Bower (1998) Role of afferents in the development and cell survival of the vertebrate nervous system. *Clin. Exp. Pharmacol. Physiol.* **25**, 487-495.

Sherren N and BA Pappas (2005) Selective acetylcholine and dopamine lesions in neonatal rats produce distinct patterns of cortical dendritic atrophy in adulthood. *Neuroscience* **136**, 445-456.

Shirvan A, I Ziv, G Fleminger, R Shina, Z He, I Brudo, E Melamed and A Barzilai (1999) Semaphorins as mediators of neuronal apoptosis. *J. Neurochem.* **73**, 961-971.

Sullivan RM and W Brake (2003) What the rodent cortex can teach us about attention deficit/hyperactivity disorder: the critical role of early deveopmental events on prefrontal function. *Behav. Brain Res.* **146**, 43-55.

Thinus-Blanc C, E Save, C Rossi-Arnaud, A Tozzi and M Ammassari-Teule (1996) The difference shown by C57BL/6 and DBA/2 inbred mice in detecting spatial novelty are subserved by a different hippocampal and parietal cortex interplay. *Behav. Brain Res.* **80**, 33-40.

Valpuesta JM, J Martin-Benito, P Gomez-Puertas, JL Carrascosa and KR Willison (2002) Structure and function of a protein folding machine: the eukaryotic cytosolic chaperonin CCT. *FEBS Lett.* **529**, 11-16.

Vinh DB and DG Drubin (1994) A yeast TCP-1-like protein is required for actin function *in vivo. Proc. Natl. Acad. Sci. USA* **91**, 9116-9120.

Weinstein B and F Solomon (1990) Phenotypic consequences of tubulin overproduction in *Saccharomyces cerevisiae*: differences between α-tubulin and β-tubulin. *Mol. Cell. Biol.* **10**, 5295-5304.

Wong WT, BE Faulkner-Jones, JR Sanes and RO Wong (2000) Rapid dendritic remodeling in the developing retina: dependence on neurotransmission and reciprocal regulation by Rac and Rho. *J. Neurosci.* **20**, 5024-5036.

Woolsey TA and H Van der Loos (1970) The structural organization of layer IV in the somatosensory region (SI) of mouse cerebral cortex. *Brain Res.* **17**, 205-242.

Ziv NE and CC Garner (2004) Cellular and molecular mechanisms of presynaptic assembly. *Nat. Rev. Neurosci.* **5**, 385-399.

Supplementary Table I. Functional classification of transcripts whose expression was changed after 6-OHDA treatment

GenBank#	Gene Name	Symbol	Control Means ± SE	6-OHDA Means ± SE	*p* values
		Differentiation and Synaptogenesis			
Up-regulated					
BQ551360	semaphorin 3A	Sema3A	0.76 ± 0.11	1.29 ± 0.17	0.031
BG065384	GABA(A) receptor-associated protein 2	GABARAP2	0.83 ± 0.21	1.78 ± 0.39	0.041
BG084093	N-myc downstream regulated 2	NDRG2	0.80 ± 0.09	1.38 ± 0.18	0.015
Down-regulated					
BG082125	embryonic lethal abnormal vision like 2 (HuB)	ELAVL2/HuB	1.43 ± 0.20	0.77 ± 0.12	0.015
AW538347	E2F transcription factor 4	E2F4	1.85 ± 0.50	0.81 ± 0.12	0.019
BG064751	E4F transcription factor 1	E4F1	1.21 ± 0.14	0.75 ± 0.09	0.037
BG063079	adrenomedullin	ADM	2.10 ± 0.88	0.63 ± 0.11	0.039
BG076926	synaptophysin-like protein 1	Sypl	2.17 ± 0.53	0.82 ± 0.08	0.012
		Cytoskeleton			
Up-regulated					
BG087420	tubulin beta 5	Tubb5	0.88 ± 0.08	1.34 ± 0.17	0.028
BG084568	tubulin cofactor a	Tbca	0.66 ± 0.08	1.29 ± 0.10	0.000
BQ551468	tubulin delta 1	Tubd1	0.88 ± 0.06	1.51 ± 0.25	0.024
AU041357	ras homolog D (RhoD)	RhoD	0.91 ± 0.08	1.29 ± 0.1 3	0.036
BQ551751	ankyrin 3, epithelial	Ank3	0.81 ± 0.07	1.55 ± 0.25	0.006
BG072071	cell division cycle 42 homolog	Cdc42	0.89 ± 0.10	1.47 ± 0.23	0.034
BG085359	peroxisomal farnesylated protein	Pxf	0.82 ± 0.06	1.76 ± 0.52	0.020
	nuclear autoantigen	Gs2na-pending	0.94 ± 0.12	1.28 ± 0.11	0.048
BG075073	thymosin, beta 4, X chromosome	Tmsb4x	0.85 ± 0.11	1.30 ± 0.21	0.049
BQ550549	vasodilator-stimulated phosphoprotein	Vasp	0.86 ± 0.08	1.20 ± 0.07	0.010
Down-regulated					
BG064770	chaperonin subunit 5 (epsilon)	CCT5	1.36 ± 0.17	0.72 ± 0.10	0.015
BQ550999	chaperonin subunit 6a (zeta)	CCT6a	1.65 ± 0.42	0.58 ± 0.19	0.007
BG063426	keratin complex 2, basic, gene 7	Krt2-7	1.11 ± 0.07	0.76 ± 0.12	0.045
BG077718	protein tyrosine kinase 9	Ptk9	1.42 ± 0.26	0.81 ± 0.10	0.031
		Apoptosis			
Up-regulated					
BC064681	glyceraldehyde-3-phosphate dehydrogenase	GAPDH	0.78 ± 0.38	1.91 ± 0.37	0.015
BG086000	insulin-like growth factor 2, binding protein 1	IGF2BP1	0.80 ± 0.10	1.54 ± 0.22	0.007
BG088461	nerve growth factor receptor associated protein 1	NGFRAP1	0.83 ± 0.08	1.32 ± 0.19	0.04
BG086002	granule-associated protein of cytotoxic T cells	TIA-1	0.82 ± 0.08	1.16 ± 0.12	0.035
Down-regulated					
BG080846	Jun oncogene	c-Jun	1.33 ± 014	0.82 ± 0.13	0.019
BG080755	myocyte enhancer factor 2D	MEF2D	1.48 ± 0.22	0.92 ± 0.15	0.040
BG077865	TNF superfamily, member 5-induced protein 1	TNFSF5IP1	1.35 ± 0.20	0.84 ± 0.10	0.037
BG077775	TNF receptor superfamily, member 23	TNFRSF23	1.39 ± 0.18	0.70 ± 0.12	0.007
BG069346	eyes absent 2 homolog	Eya2	1.20 ± 0.15	0.74 ± 0.11	0.023
		Transcription			
Up-regulated					
BQ550532	nuclear factor of kappa light polypeptide gene enhancer in B-cells 2, p49/p100	NFkB2	0.94 ± 0.09	1.31 ± 0.14	0.034
BQ551270	AE binding protein 1	Aebp1	0.79 ± 0.11	1.42 ± 0.23	0.045
BG071774	Ly1 antibody reactive clone	Lyar	0.86 ± 0.07	1.66 ± 0.43	0.040
BQ550072	Mblk1-related protein-2	Mlr2	0.80 ± 0.14	1.28 ± 0.16	0.026
BG084781	metastasis associated 3	Mta3	0.82 ± 0.08	1.38 ± 0.13	0.004
BQ550910	neural-salient serine/arginine-rich	Nssr	0.72 ± 0.06	1.87 ± 0.29	0.0001
BG075327	nuclear receptor co-repressor 1	Ncor1	0.80 ± 0.08	1.41 ± 0.18	0.005
BG087125	nuclear receptor subfamily 0 group B member 2	Nr0b2	0.91 ± 0.10	1.54 ± 0.22	0.022

Supplementary Table I. Functional classification of transcripts whose expression was changed after 6-OHDA treatment

GenBank#	Gene Name	Symbol	Control Means ± SE	6-OHDA Means ± SE	*p* values
Down-regulated					
BG063556	Bcl6 interacting corepressor	Bcor	1.48 ± 0.39	0.76 ± 0.21	0.046
BG065267	brachyury	T	1.27 ± 0.10	0.70 ± 0.12	0.009
BG078364	E26 avian leukemia oncogene 1, 5' domain	Ets1	1.46 ± 0.19	0.73 ± 0.09	0.004
BG064857	CCAAT/enhancer binding protein alpha (C/EBP)	Cebpa-rs1	1.61 ± 0.30	0.78 ± 0.18	0.022
BG079290	GATA binding protein 1	GATA1	1.38 ± 0.17	0.74 ± 0.31	0.030
AU015927	general transcription factor III C 1	Gtf3c1	1.45 ± 0.19	0.76 ± 0.09	0.004
BG077101	hairy/enhancer-of-split related with YRPW motif	Heyl	1.26 ± 0.12	0.83 ± 0.15	0.037
BG080836	homeodomain interacting protein kinase	Hipk3	1.38 ± 0.19	0.86 ± 0.11	0.032
BG082595	LIM domain binding 1	Ldb1	1.24 ± 0.14	0.74 ± 0.15	0.025
BG077936	metal response element binding transcription factor	Mtf1	1.48 ± 0.29	0.85 ± 0.12	0.043
BG069165	prolactin regulatory element binding	Preb	1.60 ± 0.37	0.81 ± 0.11	0.032
BG064938	RD RNA-binding protein	Rdbp	1.18 ± 0.10	0.62 ± 0.12	0.016
BG088179	SET domain, bifurcated 1	Setdb1	1.22 ± 0.10	0.58 ± 0.15	0.020
BG075593	TAF12 RNA polymerase II, TATA box binding protein	Taf12	1.23 ± 0.10	0.59 ± 0.17	0.019
BG085163	TATA box binding protein RNA polymerase I, A	Taf1a	1.32 ± 0.15	0.65 ± 0.21	0.011
BG088746	tripartite motif protein 27	Trim27	1.28 ± 0.15	0.59 ± 0.17	0.026
BG088173	tudor domain containing 1	Tdrd1	1.30 ± 0.12	0.61 ± 0.19	0.036
		Translation			
Up-regulated					
BG084444	eukaryotic translation elongation factor 1 epsilon 1	Eef1e1	0.83 ± 0.06	2.27 ± 0.59	0.003
BG072533	heterogeneous nuclear ribonucleoprotein A1	Hnrpa1	0.83 ± 0.09	1.30 ± 0.14	0.022
BQ550908	poly (A) polymerase alpha	Papola	0.85 ± 0.05	1.70 ± 0.26	0.004
BG072137	transcription factor B2, mitochondrial	Tfb2m	0.88 ± 0.07	2.36 ± 0.69	0.030
BG088199	5'-3' exoribonuclease 2	Xrn2	1.29 ± 0.13	0.69 ± 0.14	0.046
Down-regulated					
BG077690	basic leucine zipper and W2 domains 2	Bzw2	1.33 ± 0.16	0.89 ± 0.12	0.044
BG064782	DEAD (Aas-Glu-Ala-Asp) box polypeptide 5	Ddx5	1.11 ± 0.07	0.76 ± 0.10	0.023
BG077018	eukaryotic translation initiation factor 1A	EIF1A	1.27 ± 0.19	0.69 ± 0.13	0.017
BG077750	eukaryotic translation initiation factor 3	EIF3	1.34 ± 0.18	0.79 ± 0.12	0.047
BG064923	eukaryotic translation initiation factor 3 subunit 2	EIF3S2	1.30 ± 0.23	0.75 ± 0.18	0.042
BG078361	eukaryotic translation initiation factor 4 gamma 2	EIF4G2	1.52 ± 0.21	0.88 ± 0.11	0.033
BG063771	poly A binding protein, cytoplasmic 1	Pabpc1	1.46 ± 0.14	0.80 ± 0.08	0.003
BG077146	seryl-aminoacyl-tRNA synthetase 1	Sars1	1.20 ± 0.15	0.67 ± 0.13	0.025
		Protein Synthesis			
Up-regulated					
BQ552082	carboxypeptidase X 1	Cpx1	0.94 ± 0.13	1.91 ± 0.45	0.047
AB030378	chondroitin 4-sulfotransferase 2	C4st2	0.73 ± 0.12	1.28 ± 0.18	0.024
BG072192	alpha-N-acetylglucosaminidase	Naglu	0.92 ± 0.07	1.38 ± 0.18	0.027
BG087134	D-dopachrome tautomerase	Ddt	0.85 ± 0.10	1.39 ± 0.24	0.048
BQ551115	geranylgeranyl diphosphate synthase 1	Ggps1	0.84 ± 0.11	1.38 ± 0.21	0.026
AW558740	mannosidase 1, beta	Man1b	0.63 ± 0.13	2.18 ± 0.67	0.014
BG076333	methylenetetrahydrofolate dehydrogenase	Mthfd2	0.81 ± 0.09	1.30 ± 0.20	0.027
BG084015	phosphoserine aminotransferase 1	Psat1	0.78 ± 0.10	1.69 ± 0.47	0.024
AU043387	proteasome 26S subunit, non-ATPase, 12	Psmd12	0.79 ± 0.18	1.56 ± 0.32	0.030
BC001982	proteasome subunit, alpha type 4	Psma4	0.79 ± 0.10	1.85 ± 0.35	0.008
BG071790	protein phosphatase 1, gamma isoform	Ppp1cc	0.88 ± 0.07	1.27 ± 0.17	0.034
BG074107	ribosomal protein L3	Rpl3	0.87 ± 0.11	1.62 ± 0.29	0.027
BC054388	ribosomal protein L37a	Rpl37a	0.85 ± 0.09	1.39 ± 0.21	0.047
BG084847	ribosomal protein L39	Rpl39	0.81 ± 0.13	1.86 ± 0.37	0.007
BG072802	ribosomal protein S16	Rps16	0.86 ± 0.07	1.54 ± 0.28	0.036
AW556256	ribosomal protein S6	Rps6	0.91 ± 0.05	1.33 ± 0.18	0.046
BG086349	ring finger protein 11	Rnf11	0.88 ± 0.15	1.45 ± 0.22	0.041
BQ552743	RNA binding protein gene	Rbpms	0.88 ± 0.11	1.41 ± 0.20	0.024
BG070610	SUMO/serine specific protease 3	Snp3	0.89 ± 0.10	1.45 ± 0.26	0.033

Supplementary Table I. Functional classification of transcripts whose expression was changed after 6-OHDA treatment

GenBank#	Gene Name	Symbol	Control Means ± SE	6-OHDA Means ± SE	*p* values
		Protein Synthesis			
Down-regulated					
BG069982	arachidonate 12-lipoxygenase	Alox12	1.37 ± 0.20	0.73 ± 0.12	0.034
BQ551716	sialyltransferase 7B	Siat7b	1.22 ± 0.08	0.72 ± 0.15	0.024
BG076775	ubiquitin specific protease 39	Usp39	2.25 ± 0.94	0.80 ± 0.09	0.029
BG064714	solute carrier family 3 (amino acid transport) 2	Slc3a2	1.38 ± 0.21	0.76 ± 0.11	0.021
BG077813	SUMO/sentrin specific protease 6	Senp6	1.69 ± 0.30	0.76 ± 0.08	0.002
BG070343	tripartite motif protein 6	Trim6	1.33 ± 0.13	0.85 ± 0.06	0.003
BG065003	ubiquitin specific protease 21	Usp21	1.40 ± 0.23	0.77 ± 0.14	0.021
BG069818	ubiquitin specific protease 3	Usp3	1.54 ± 0.23	0.78 ± 0.11	0.005
BG075068	1,4- galactosyltransferase polypeptide 1	B4galt1	1.37 ± 0.20	0.67 ± 0.21	0.023
BG067882	component of oligomeric golgi complex 8	Cog8	1.63 ± 0.33	0.73 ± 0.14	0.008
BG077676	DnaJ (Hsp40) homolog subfamily C member 7	Dnajc7	1.27 ± 0.15	0.78 ± 0.10	0.020
BG069686	ELOVL6 elongation of long chain fatty acids	Elovl6	1.77 ± 0.34	0.90 ± 0.17	0.042
BG078410	enolase 1 alpha non-neuron	Eno1	1.34 ± 0.14	0.72 ± 0.11	0.007
AU020524	3-hydroxy-3methylglutaryl-Coenzyme A synthase	HMG-CoA synthase	1.60 ± 0.30	0.82 ± 0.15	0.047
BG078653	heterogeneous nuclear ribonucleoprotein D	Hnrpd	1.76 ± 0.33	0.90 ± 0.09	0.018
BG066944	inter-alpha trypsin inhibitor heavy chain 1	Itih1	1.49 ± 0.41	0.65 ± 0.16	0.037
BG064451	low-density lipoprotein receptor- related protein 10	Lrp10	1.26 ± 0.15	0.74 ± 0.09	0.014
BG077757	ERO1-like	Ero1l	1.40 ± 0.18	0.79 ± 0.12	0.021
BG084205	fatty acid Coenzyme A ligase long chain 5	Facl5	1.33 ± 0.14	0.68 ± 0.15	0.007
BG080374	phosphatidic acid phosphatase type 2B	Ppap2b	1.48 ± 0.18	0.62 ± 0.11	0.000
AW539280	Yip1 interacting factor homolog	Yif1	1.44 ± 0.21	0.72 ± 0.15	0.025
BG064771	glucosamine-6-phosphate deaminase	Gnpi	1.29 ± 0.17	0.71 ± 0.12	0.022
AW556794	guanosine monophosphate reductase 2	Gmpr2	1.57 ± 0.31	0.79 ± 0.11	0.011
BG074714	paraoxonase 3	Pon3	1.30 ± 0.12	0.58 ± 0.16	0.017
BG075312	Transketolase	Tkt	1.20 ± 0.10	0.79 ± 0.09	0.026
BG064680	malic enzyme	Mod1	1.24 ± 0.11	0.86 ± 0.06	0.015
BG065235	methionine aminopeptidase 2	Metap2	1.43 ± 0.23	0.77 ± 0.15	0.024
BG073306	mitochondrial ribosomal protein 1	Mrpl1	1.53 ± 0.29	0.74 ± 0.16	0.031
BG063606	NADH dehydrogenase assembly factor 1	Ndufaf1	1.41 ± 0.21	0.84 ± 0.12	0.041
BG077408	phosphomannomutase 1	Pmm1	1.70 ± 0.41	0.82 ± 0.12	0.046
C75970	protein phosphatase 2a beta	PPP2Ab	1.37 ± 0.20	0.83 ± 0.11	0.049
BG068173	protein tyrosine phosphatase 4a1	PTP4A1	1.15 ± 0.11	0.73 ± 0.14	0.027
BG065196	ribosomal protein L5	Rpl5	1.75 ± 0.44	0.79 ± 0.14	0.019
BG063883	ribosomal protein L7	Rpl7	1.99 ± 0.57	0.90 ± 0.13	0.039
BG077480	ribosomal protein L8	Rpl8	1.29 ± 0.17	0.73 ± 0.11	0.018
BG063083	ribosomal protein S6 kinase polypeptide 2	Rps6ka2	1.41 ± 0.16	0.87 ± 0.07	0.006
BG077478	serine protease inhibitor 6	Spi6	1.59 ± 0.30	0.76 ± 0.15	0.010
		Signal transduction			
Up-regulated					
BQ552159	ankyrin repeat and SOCS box-protein 6	Asb6	0.83 ± 0.07	1.24 ± 0.11	0.006
BQ552281	annexin A6	Anxa6	0.86 ± 0.11	1.64 ± 0.35	0.046
BQ551016	homer, neuronal immediate early gene	Homer3	0.82 ± 0.10	1.33 ± 0.16	0.014
BG087137	kit oncogene	Kit	0.72 ± 0.16	1.76 ± 0.57	0.031
BQ551164	PAS serine/threonine kinase	PASK	0.86 ± 0.11	2.34 ± 0.53	0.016
BQ551079	protein phosphatase 2 subunit B	PPP2r2a	0.89 ± 0.07	1.86 ± 0.40	0.020
BG080166	RAB, member of RAS oncogene family-like 3	Rabl3	0.85 ± 0.18	2.12 ± 0.57	0.039
BQ552129	wingless-related MMTV integration site 5B	Wnt5b	0.91 ± 0.09	1.25 ± 0.11	0.048

Supplementary Table I. Functional classification of transcripts whose expression was changed after 6-OHDA treatment

GenBank#	Gene Name	Symbol	Control Means ± SE	6-OHDA Means ± SE	*p* values
		Signal transduction			
Down-regulated					
BG088471	B-cell receptor-associated protein 29	Bcap29	1.24 ± 0.10	0.80 ± 0.09	0.007
BC054805	calmodulin 1	Calm1	1.45 ± 0.19	0.91 ± 0.12	0.039
AW554667	constitutive photomorphogen 9 subunit 5	Cops5	1.27 ± 0.12	0.64 ± 0.17	0.028
BG064928	disabled homolog 2 (Drosophila)	Dab2	1.36 ± 0.29	0.78 ± 0.11	0.038
BG065213	growth factor receptor bound protein 10	Grb10	1.27 ± 0.14	0.87 ± 0.11	0.041
BG078399	guanine nucleotide binding protein beta 2	Gnb2	1.40 ± 0.19	0.73 ± 0.15	0.022
BG064826	HS1 binding protein	Hs1bp1	1.40 ± 0.28	0.78 ± 0.14	0.043
BG081243	inositol 1,4,5-triphosphate receptor 1	Itpr1	1.56 ± 0.37	0.80 ± 0.20	0.045
BG063736	nemo like kinase	Nlk	1.38 ± 0.21	0.85 ± 0.11	0.049
BG071651	RAB11a, member RAS oncogene family	Rab11a	2.01 ± 0.56	0.68 ± 0.19	0.010
BG080845	related RAS viral (r-ras) oncogene 2	Rras2	1.48 ± 0.22	0.68 ± 0.17	0.008
BG077776	serine/threonine kinase 10	Stk10	1.45 ± 0.24	0.74 ± 0.10	0.013
BQ551075	SH3-domain binding protein 1	Sh3bp1	0.89 ± 0.07	0.58 ± 0.26	0.015
BG079034	sphingosine kinase 2	Sphk2	1.60 ± 0.24	0.67 ± 0.17	0.005
BG070360	suppressor of cytokine signaling 4	Socs4	1.24 ± 0.13	0.73 ± 0.13	0.018
L33417	very low density lipoprotein receptor	Vldlr	1.52 ± 0.29	0.71 ± 0.15	0.029
		Intracellular transport			
Up-regulated					
AU042390	ATPase, Ca++ transporting, slow twitch 2	Atp2a2	0.72 ± 0.09	1.49 ± 0.35	0.030
BQ552336	ATPase, Cu++ transporting, alpha polypeptide	Atp7a	0.80 ± 0.15	1.53 ± 0.34	0.044
BG085675	ATPase, H+ transporting, lysosomal	Atp6g1	0.85 ± 0.08	1.61 ± 0.24	0.007
BG087256	ATP-binding cassette, subfamily E member 1	Abce1	0.86 ± 0.08	1.45 ± 0.22	0.018
BG072229	calbindin-28K	Calb1	0.86 ± 0.11	1.67 ± 0.37	0.032
BG086010	dynein, cytoplasmic, intermediate chain 2	Dncic2	0.79 ± 0.10	1.71 ± 0.29	0.011
BG085334	SAR1a gene homolog	Sara1	0.82 ± 0.11	1.17 ± 0.08	0.046
BG083967	sideroflexin 1	Sfxn1	0.82 ± 0.09	1.30 ± 0.19	0.047
BG087217	sideroflexin 3	Sfxn3	0.87 ± 0.12	1.39 ± 0.19	0.044
BG084323	solute carrier family 34	Slc34a2	0.77 ± 0.08	1.59 ± 0.27	0.009
BQ552559	solute carrier family 6	Slc6a6	0.86 ± 0.08	1.55 ± 0.22	0.009
BG088027	striatin, calmodulin binding protein 3	Strn3	0.94 ± 0.12	1.28 ± 0.11	0.048
BG071195	Vitelliform macular dystrophy 2	Vmd2	0.84 ± 0.10	2.13 ± 0.65	0.036
BQ551106	Tyr3/Trp5-monooxygenase activation protein	Ywhab	0.87 ± 0.15	1.47 ± 0.19	0.018
BC047281	1-acylglycerol-3-phosphate O- acyltransferase 1	Agpat4	0.85 ± 0.12	1.26 ± 0.11	0.034
		Intracellular transport			
Down-regulated					
BG064835	a disintegrin-like and metalloprotease	Adamts10	1.42 ± 0.15	0.74 ± 0.1	0.006
BG078400	adaptor protein complex AP-1 mu 2	Ap1m2	1.36 ± 0.16	0.75 ± 0.12	0.018
BG077736	aldehyde dehydrogenase 9 subfamily A1	Aldh9a1	1.43 ± 0.22	0.88 ± 0.10	0.048
BG076762	ATPase, Na+/K+ transporting beta 1	Atp1b1	1.35 ± 0.21	0.78 ± 0.12	0.034
BG064795	ferritin light chain 1	Ftl1	1.33 ± 0.16	0.83 ± 0.13	0.042
BG085818	hemoglobin alpha adult chain 1	Hba-a1	1.24 ± 0.12	0.75 ± 0.16	0.029
BG085146	lactotransferrin	Ltf	1.17 ± 0.05	0.59 ± 0.13	0.046
BG088166	lysosomal apyrase-like 1	Lysal1	1.20 ± 0.08	0.75 ± 0.09	0.008
BQ551346	Mucolipin 3	Mcoln3	0.72 ± 0.09	1.38 ± 0.21	0.007
BG064735	peroxiredoxin 5	Prdx5	1.31 ± 0.19	0.80 ± 0.15	0.038
BG069106	potassium voltage-gated channel H member 1	Kcnh1	1.43 ± 0.27	0.79 ± 0.10	0.038
BG064853	monocarboxylate transporter 4	MCT4	1.33 ± 0.12	0.80 ± 0.14	0.015
BG072114	solute carrier 21 prostaglandin transporter 2	Slc21a2	1.15 ± 0.09	0.64 ± 0.17	0.040
BG085151	solute carrier 27 fatty acid transporter 4	Slc27a4	1.31 ± 0.10	0.62 ± 0.15	0.028
BG075243	solute carrier 30 zinc transporter 3	Slc30a3	1.43 ± 0.21	0.85 ± 0.18	0.028
BG080898	transient receptor potential cation channel M7	Trpm7	1.78 ± 0.36	0.92 ± 0.22	0.049
BG069221	T-cell immunoglobulin and mucin domain 2	Tim-2	1.76 ± 0.43	0.93 ± 0.15	0.045

Supplementary Table I. Functional classification of transcripts whose expression was changed after 6-OHDA treatment

GenBank#	Gene Name	Symbol	Control Means ± SE	6-OHDA Means ± SE	*p* values
		Mitochondria			
Up-regulated					
BG073437	ATP synthase, H+ transporting mitochondrial beta	Atp5b	0.92 ± 0.06	1.38 ± 0.19	0.031
BG085306	cytochrome *c* oxidase, subunit VIc	COX6C	0.92 ± 0.05	2.08 ± 0.62	0.037
BG087498	electron transferring flavoprotein, alpha	Etfa	0.90 ± 0.10	1.99 ± 0.51	0.035
BQ552525	Mitochondrial ribosomal protein L45	Mrpl45	0.85 ± 0.06	1.69 ± 0.46	0.036
BC024673	NADH dehydrogenase (ubiquinone) 1 alpha 8	Ndufa8	0.83 ± 0.10	1.26 ± 0.16	0.029
Down-regulated					
BG078689	ATP synthase H+ transporting mito alpha 1	Atp5a1	1.47 ± 0.22	0.88 ± 0.10	0.031
AW537398	ATPase, H+ transporting, V1C1	Atp6v1c1	1.25 ± 0.19	0.73 ± 0.19	0.035
BG076653	benzodiazepine receptor, peripheral	Bzrp	1.65 ± 0.30	0.83 ± 0.08	0.013
BG076988	cytochrome c oxidase, subunit VIIIa	COX8A	1.14 ± 0.09	0.75 ± 0.16	0.041
BG073306	mitochondrial ribosomal protein L1	Mrpl1	1.53 ± 0.29	0.74 ± 0.16	0.031
BQ550897	NADH dehydrogenase (ubiquinone) 1 alpha 10	Ndufa10	1.31 ± 0.14	0.68 ± 0.19	0.025
BG063606	NADH dehydrogenase (ubiquinone) 1 alpha	Ndufaf1	1.41 ± 0.21	0.84 ± 0.12	0.041
		Cell Adhesion			
Up-regulated					
BG075757	CD 81 antigen	CD81	0.76 ± 0.12	1.28 ± 0.17	0.018
BG075779	procollagen, type VI alpha 1	Col6a1	0.75 ± 0.12	1.60 ± 0.43	0.045
BG076147	elastin microfibril interfacer 3	lipin 3/Emilin3	0.85 ± 0.08	1.44 ± 0.19	0.013
BQ552186	procollagen, type V alpha 1	Col5a1	0.78 ± 0.20	1.74 ± 0.50	0.044
BG073805	nischarin	Nisch	0.79 ± 0.12	1.96 ± 0.51	0.022
BG088919	selectin, endothelial cell, ligand	Selel	0.75 ± 0.11	1.92 ± 0.52	0.046
		Cell Adhesion			
Down-regulated					
BG085432	chondroitin sulfate proteoglycan 6	Cspg6	1.21 ± 0.13	0.81 ± 0.10	0.038
BG069861	craniofacial development protein 1	Cfdp	1.87 ± 0.46	0.65 ± 0.14	0.012
BQ551553	lysyl oxidase-like 3	Loxl3	1.36 ± 0.18	0.84 ± 0.13	0.042
BG063694	vinculin	Vcl	1.38 ± 0.18	0.90 ± 0.11	0.046
		Cell cycle			
Up-regulated					
BQ551224	cell division cycle 71 homolog like 1	Cdc7l1	0.80 ± 0.10	1.42 ± 0.31	0.048
BQ550528	cyclin E2	Ccne2	0.89 ± 0.10	1.25 ± 0.14	0.044
BG083664	cyclin L1	Ccnl1	0.86 ± 0.09	1.81 ± 0.49	0.048
BG086478	G1 to phase transition 1	Gspt1	0.89 ± 0.07	2.37 ± 0.79	0.034
BG075056	telomerase associated protein 1	Tep1	0.75 ± 0.14	1.25 ± 0.15	0.039
		Cell cycle			
Down-regulated					
BG063118	inner centromere protein	Incenp	1.55 ± 0.23	0.79 ± 0.09	0.008
BG064865	mini chromosome maintenance deficient 5	Mcm5	1.46 ± 0.27	0.80 ± 0.19	0.042
BG066368	checkpoint kinase 1 homolog	Chek1	1.62 ± 0.31	0.72 ± 0.13	0.039
		Growth factors			
Up-regulated					
BQ551034	Bone morphogenetic protein 8b	BMP8b	0.83 ± 0.08	1.42 ± 0.21	0.021
BG088057	Glia maturation factor beta	GMFB	0.95 ± 0.07	1.31 ± 0.15	0.046
AU040433	Transforming growth factor alpha	TGFa	0.79 ± 0.09	1.73 ± 0.33	0.010
Down-regulated					
BC052677	Growth differentiation factor 9	GDF9	1.45 ± 0.34	0.73 ± 0.13	0.032

Supplementary Table I. Functional classification of transcripts whose expression was changed after 6-OHDA treatment

GenBank#	Gene Name	Symbol	Control Means ± SE	6-OHDA Means ± SE	*p* values
		DNA damage / Stress response proteins			
Up-regulated					
BG071480	DNA polymerase epsilon subunit 2	Pole2	0.87 ± 0.06	1.46 ± 0.25	0.011
BG076183	Structural maintenance of chromosomes 1	SMC1	0.78 ± 0.10	1.54 ± 0.18	0.005
BG077269	Structural maintenance of chromosomes 4	SMC4	0.77 ± 0.16	2.48 ± 0.61	0.028
BG071892	RAD21 homolog	RAD21	0.83 ± 0.13	1.61 ± 0.27	0.021
BQ552179	REV3-like DNA polymerase zeta	Rev3l	0.83 ± 0.10	1.33 ± 0.16	0.025
BG085381	Degenerative spermatocyte homolog	Degs	0.83 ± 0.07	1.45 ± 0.23	0.011
BC030444	Glutathione S-transferase, mu 4	Gstm4	0.85 ± 0.12	1.77 ± 0.38	0.038
BG074109	Heat shock protein, 86 kDa 1	Hsp86-1	0.86 ± 0.07	1.56 ± 0.42	0.041
BG087426	Heat shock 70kD protein 8	Hspa8	0.87 ± 0.08	1.42 ± 0.17	0.019
BG072457	Myotrophin	Mtpn	0.89 ± 0.10	1.56 ± 0.23	0.019
Down-regulated					
BC034517	excision repair cross-complementing group 2	Ercc2	1.42 ± 0.20	0.69 ± 0.09	0.002
BG088755	DnaJ (Hsp40) homolog, subfamily A member 1	Dnaja1	1.20 ± 0.10	0.78 ± 0.11	0.049
BG065483	DnaJ (Hsp40) homolog, subfamily B member 1	Dnajb1	1.63 ± 0.27	0.86 ± 0.14	0.031
		Unclassified/Other			
Up-regulated					
BG071424	integral membrane protein 2C	Itm2C	0.78 ± 0.12	1.28 ± 0.20	0.035
Down-regulated					
BG064201	Ewing sarcoma homolog	Ewsh	1.51 ± 0.31	0.76 ± 0.12	0.026
C86521	f-box only protein 32	Fbxo32	1.34 ± 0.17	0.77 ± 0.13	0.026
BQ551727	unc-84 homolog A	Unc84a	1.21 ± 0.15	0.60 ± 0.18	0.014